South East Asian J. of Mathematics and Mathematical Sciences
Vol. 21, No. 3 (2025), pp. 313-348

DOI: 10.56827/SEAJMMS.2025.2103.19 **ISSN (Online): 2582-0850**

ISSN (Print): 0972-7752

UNSTEADY SECOND GRADE ALIGNED MHD FLUID THROUGH POROUS MEDIA IN A ROTATING FRAME: A CLASS OF EXACT SOLUTIONS USING INVERSE METHOD

Birendra Kumar Vishwakarma and Sayantan Sil*

University Department of Physics,
BBMK University,
Dhanbad - 826004, Jharkhand, INDIA

E-mail : biru12maths@gmail.com

*Department of Physics,
P.K. Roy Memorial College,
Dhanbad - 826004, Jharkhand, INDIA

E-mail : sayan12350@gmail.com

(**Received:** *Apr. 03, 2025* **Accepted:** *Dec. 17, 2025* **Published:** *Dec. 30, 2025)*

Abstract: This study presents exact analytical solutions for the unsteady plane flow of an electrically conducting second-grade fluid within a rotating frame, permeating a porous medium under the action of a magnetic field. The analysis employs the inverse method, wherein suitable *a priori* assumptions for the vorticity and stream function yield consistent forms of the velocity field and pressure distribution. Closed-form expressions for the governing flow variables are derived, ensuring compliance with both the fundamental equations and physical constraints. The influence of critical parameters, such as rotational effects, magnetic field intensity, porous medium resistance, and non-Newtonian fluid characteristics, is examined in detail. Graphical illustrations highlight the role of these parameters in shaping the flow dynamics, offering deeper insight into the complex interplay between rotation, magnetohydrodynamic forces, and porous medium interactions.

Keywords and Phrases: MHD, porous medium, inverse method, exact solution, stream function, unsteady flow.

2020 Mathematics Subject Classification: 76B75, 76D55, 76N25.

1. Introduction

We have observed that there are several notable applications of magnetohydrodynamics (MHD) in industrial sectors, science, and engineering, apart from that the study of MHD fluid flow has earned remarkable attention in the dynamics of fluid fraternity. We can find the implementation of such important aspects in the study regarding nuclear fuel debris, solidification processes of metal alloys and metals, the control of underground spreading of chemical wastes and pollution and the design of MHD power generators and to understand the theory of geophysics and astrophysics.

To explain the flow behavior of electrically conducting fluids, we need to solve the governing magnetohydrodynamic (MHD) equations that arise in such fluids. These equations are crucial because they apply to various fluid flows, from thin films to large-scale atmospheric phenomena. However, their non-linear nature presents challenges in obtaining exact solutions. As a result, the full set of general solutions for MHD equations remains an open problem. To address this difficulty, many researchers have explored transformations and inverse or semi-inverse methods to reformulate these equations into a solvable form. Ames [2] was the first to transform non-linear partial differential equations into a solvable form.

The concept of rotating fluids has garnered substantial importance across a wide array of scientific, engineering, and product applications. These applications span from the design and modeling of jet engines, pumps, and vacuum cleaners to the study of geophysical flows. Extensive research has been conducted on rotating fluids, and numerous investigations [14], [29], [33], [36], [37], [39], and [41] have explored various types of flows.

Exact solutions to the Navier-Stokes equations are limited in number and become even scarcer when considering non-Newtonian constitutive equations [31]. This scarcity is due to the non-linear nature of these equations, which makes them difficult to solve exactly. To address these challenges, researchers have employed the inverse method to solve various flow problems. For homogeneous incompressible fluids of the second grade [3], [5], [6], [7], [27] the governing equations are generally of third order, unlike the second-order Navier-Stokes equations. Thus, in addition to the perturbation approach, an extra boundary condition is usually required beyond those used for solving the Navier-Stokes equations. The inverse method helps avoid the need for this additional condition, making it an attractive approach for studying non-Newtonian fluids. This method involves making certain *a priori* assumptions about the forms of the velocity field and pressure without any assumptions about the boundaries of the fluid domain. These assumptions are often made about the velocity field and rarely about the pressure. By assuming

that vorticities are proportional to the stream function, Taylor [40] obtained a solution for a double-infinite array of vorticities decaying exponentially over time. This method has been widely used by many researchers for first-grade fluids, including Kovasznay [17], Wang [45] - [46], Lin and Tobak [44], Ridha [30], Hui [12], Jeffery [15], Kumar [18], [19], Labropulu [20], [21], [22], Chandna and Oku-Ukpong [8] and others. These researchers assumed that the vorticity is proportional to the stream function perturbed by a uniform stream and derived several classes of exact solutions. Using the same technique, [25], [26], [32] obtained some inverse solutions for incompressible couple stress fluid flow.
Significant research has been conducted by various researchers [4], [24], [42], [43] on flow through porous media and in a rotating reference frame. Bhatt and Shirley [4] investigated various types of flows through porous media and rotating reference frames. Singh et al. [34] applied this method to find exact solutions for MHD rotating flows in porous media.

Gupta [11] derived exact solutions for steady three-dimensional Navier-Stokes equations for the flow past a porous plate in a rotating frame of reference. Soundalgekar and Por [39] examined hydromagnetic flow in a rotating fluid past an infinite porous wall. Singh et al. [28], [34] studied steady plane flows of an incompressible rotating viscous fluid with infinite electrical conductivity. Singh and Thakur [35] investigated variably inclined MHD flows through porous media in the magnetograph plane. Various analytical and numerical studies in the literature, both non-MHD and MHD, have been conducted for unsteady or time-dependent flows of different natures. Ram and Mishra studied unsteady MHD flow through porous media. Rashid [29] elucidated the effect of radiation and variable viscosity on unsteady MHD flow of a rotating fluid from a stretching surface in porous media. Recently, various studies has been done on MHD in porous media and second-grade fluids some of them [1], [9], [10], [16], [13], [47] has rigorously examined MHD unidirectional motions of incompressible second-grade fluids through a porous medium, proving structural similarities in the governing equations for velocity and shear stress and offering analytical insights into these flows

This present work is divided into several sections, in section 2 the governing equations for the unsteady flow of an incompressible second-grade fluid in a rotating frame are formulated by incorporating magnetic field effects, porous medium resistance, and non-Newtonian stress terms. Appropriate assumptions and nondimensional variables are introduced to simplify the model. In section 3 the inverse method has been used to determine exact solutions for the unsteady plane, second grade, aligned electrically conducting MHD fluid in a rotating frame through porous media in the presence of a magnetic field. In sections 4, 5 and 6 exact solutions are obtained by assuming forms of the vorticity function *a priori* and the stream function *a priori*. The expressions for velocity components, magnetic field components, stream function, and vorticity functions are derived for both steady and unsteady cases. Also this section analyzes the effects of key physical parameters such as rotation, magnetic field strength, porous medium resistance, and second-grade fluid parameter on streamline patterns and the velocity profiles. The results are presented graphically and discussed in comparison with classical Newtonian and non-rotating cases. Section 7 contains the main findings of the study are summarized, highlighting the stabilizing effects of rotation and magnetic fields and the influence of non-Newtonian characteristics. Possible extensions of the present work are suggested for future research. The present analysis is more general, and the results of F. Labropulu [23] and Manoj Kumar, Sayantan Sil, and C. Thakur [38] can be recovered in the limiting case.

2. Equation of Motion

The equations of motion for an unsteady, second-grade, incompressible, viscous, and electrically conducting fluid in a rotating frame, traversing through a porous medium under the influence of a magnetic field, are

$$\nabla \cdot \overrightarrow{V} = 0, \tag{1}$$

$$\rho\Big(\frac{\partial \overrightarrow{V}}{\partial t} + 2\overrightarrow{\Omega} \times V + \overrightarrow{\Omega} \times \overrightarrow{\Omega} \times \overrightarrow{r} + (\overrightarrow{V} \cdot \nabla)\overrightarrow{V}\Big) = \nabla \cdot \mathbf{T} + \rho f + \mu^*(\nabla \times \overrightarrow{H}) \times \overrightarrow{H} - \frac{\phi^*}{k}(\mu + \alpha_1 \frac{\partial}{\partial t})\overrightarrow{V}, \tag{2}$$

$$\frac{\partial H}{\partial t} = \nabla \times (\overrightarrow{V} \times \overrightarrow{H}) - \frac{1}{\mu^* \sigma} \nabla \times (\nabla \times \overrightarrow{H}), \tag{3}$$

$$\nabla \cdot \overrightarrow{H} = \mathbf{0}, \tag{4}$$

and the constitutive equation for the Cauchy stress $\mathbf{T}$

$$\mathbf{T} = -PI + \eta \mathbf{A}_1 + \alpha_1 \mathbf{A}_2 + \alpha_2 \mathbf{A}_1^2, \tag{5}$$

where, $\overrightarrow{V}$ = velocity field vector, P = dynamic pressure function, ρ = the constant fluid field density, $\overrightarrow{\Omega}$ = angular velocity vector, $\overrightarrow{r}$ = radius vector, f = body forced per unit mass, μ^* = magnetic permeability, ϕ^* = porosity, μ = coefficient of dynamic viscosity, k = permeability of the medium, σ = electrical conductivity, and α_1, α_2 are the normal stress moduli, I = isotropic tensor, -PI denotes the determinate spherical stress so that it become

$$-PI = \begin{pmatrix} P & 0 & 0 \\ 0 & P & 0 \\ 0 & 0 & P \end{pmatrix},$$

The Rivlin-Ericksen tensors $\mathbf{A}_1$ and $\mathbf{A}_2$ are defined as

$$\mathbf{A}_1 = \nabla\mathbf{V} + (\nabla\mathbf{V})^T, \mathbf{A}_2 = \dot{\mathbf{A}}_1 + (\nabla\mathbf{V})^{\mathbf{T}}\mathbf{A}_1 + \mathbf{A}_1(\nabla\mathbf{V}), \quad (6)$$

In this article we have considered MHD fluid in two dimensional flow where the body force is negligible, so we must have

$$\overrightarrow{V} = [u(x,y,t), v(x,y,t), 0], \quad (7)$$

$$\overrightarrow{H} = [(H_1(x,y,t), H_2(x,y,t), 0)], \quad (8)$$

and $f = 0$. Since

$$P' = P - \frac{1}{2}\rho|\Omega \times r|^2, \quad (9)$$

The above equation can be written in (x, y) plane as under

$$\frac{\partial u}{\partial x} + \frac{\partial v}{\partial y} = 0, \quad (10)$$

$$\begin{aligned}\rho(u_t + uu_x + vu_y) + P'_x = {} & \mu\nabla^2 u \\ & + \alpha_1\left\{\nabla^2 u_t + \frac{\partial}{\partial x}[2uu_x x + 2vu_x y 4{u_x}^2 2v_x(v_x + u_y)]\right\} \\ & + \alpha_1\left\{\frac{\partial}{\partial y}\Big[(u\frac{\partial}{\partial x} + v\frac{\partial}{\partial y})(v_x + u_y) + 2u_x u_y + v_x + 2v_x v_y\Big]\right\} \quad (11) \\ & + \alpha_2\left\{\frac{\partial}{\partial x}[4{u_x}^2 + (v_x + u_y)^2]\right\} - \mu^* H_2(H_2 x - H_1 y) \\ & - \frac{\phi^*}{k}\Big(\mu + \alpha_1\frac{\partial}{\partial t}\Big)u - 2\rho\Omega u,\end{aligned}$$

$$\begin{aligned}\rho(v_t + uv_x + vv_x) + P'_y &= \mu\nabla^2 v \\ &+ \alpha_1\Big\{\nabla^2 v_t + \frac{\partial}{\partial y}[2uv_xy + 2vv_yy4{v_x}^2 2u_y(v_x+u_y)]\Big\} \\ &+ \alpha_1\Big\{\frac{\partial}{\partial x}\Big[(u\frac{\partial}{\partial x} + v\frac{\partial}{\partial y})(v_x+u_y) + 2u_xu_y + v_x + 2v_xv_y\Big]\Big\} \\ &+ \alpha_2\Big\{\frac{\partial}{\partial x}[4{v_y}^2 + (v_x+u_y)^2]\Big\} \\ &+ \mu^* H_1(H_2x - H_1y) \\ &- \frac{\phi^*}{k}\Big(\mu + \alpha_1\frac{\partial}{\partial t}\Big)v - 2\rho\Omega v,\end{aligned} \tag{12}$$

$$(H_2x - H_1y)_t = \nabla^2\Big[\frac{1}{\mu^*\rho}(H_2x - H_1y) + vH_1 - uH_2\Big], \tag{13}$$

$$H_1x + H_2y = 0. \tag{14}$$

Equation (10)-(14) are five equations in five unknown functions u, v, H_1, H_2 and P' of x, y, t.
Now introducing the vorticity, current density and generalised energy function define as follows:

$$\omega = \frac{\partial v}{\partial x} - \frac{\partial u}{\partial y}, \tag{15}$$

$$J = H_2x - H_1y \tag{16}$$

$$\begin{aligned}h = P' + \frac{1}{2}\rho|\overrightarrow{\Omega}\times r|^2 + \frac{1}{2}\rho(u^2+v^2) - \alpha_1(u\nabla^2u + v\nabla^2 v) \\ -\Big(\frac{3\alpha_1 + 2\alpha_2}{2}\Big)[2{u^2}_x + 2{v^2}_y + (v_x+u_y)^2]\end{aligned} \tag{17}$$

Using equations (15) - (17), in the equations (10) - (14) we get,

$$u_x + v_y = 0 \tag{18}$$

$$h_x = -\mu\omega_y + \rho(v\omega - u_t) - \mu^* JH_2 - \alpha_1(\omega_y t + v\nabla^2\omega) + \frac{\phi^*}{k}\Big(\mu + \alpha_1\frac{\partial}{\partial t}\Big)u - 2\rho\Omega u, \tag{19}$$

$$h_y = \mu\omega_x + \rho(u\omega - v_t) + \mu^* JH_2 + \alpha_1(\omega_y t + v\nabla^2\omega) + \frac{\phi^*}{k}\Big(\mu + \alpha_1\frac{\partial}{\partial t}\Big)v - 2\rho\Omega v, \tag{20}$$

$$J_t = \nabla^2\Big(\frac{\overrightarrow{\Omega}}{\mu^*\rho} + vH_1 - uH_2\Big), \tag{21}$$

$$H_1x + H_2y = 0. \tag{22}$$

Using (18) to (22) along with (15) and (16) gives a system of seven equations in seven functions u, v,H_1, H_2, ω, J and h of x, y, t.
The continuity equation (18) implies the existence of a stream function $\psi(x, y, t)$ such that

$$u = \psi_y, v = -\psi_x. \tag{23}$$

We now study aligned flows for which the magnetic field intensity in the field of flow is everywhere parallel to velocity field. Therefore we have

$$H_1 = fu, H_2 = fv. \tag{24}$$

where$f = f(x, y, t) \neq 0$ is an arbitrary scalar function.
Now, using (23) and (24), we get

$$H_1 = f\psi_y, H_2 = -f\psi_x. \tag{25}$$

The vorticity, current density and the linear momentum equations (19) and (20) by substituting (23) and (24) can written as

$$\omega = -\nabla^2\psi, \tag{26}$$

$$J = -(f\nabla^2\psi + f_x\psi_x + f_y\psi_y), \tag{27}$$

$$\begin{aligned} h_x = \mu(\nabla^2\psi)_y + \rho(\psi_x\nabla^2\psi - (\psi_y)_t) - \mu^* f\psi_x(f\nabla^2\psi + f_x\psi_x + f_y\psi_y) \\ -\alpha_1[(\psi_x\nabla^2\psi - (\psi_y)_t)] + \frac{\phi^*}{k}(\mu + \alpha_1\frac{\partial}{\partial t})\psi_y - 2\rho\overrightarrow{\Omega}\psi_x, \end{aligned} \tag{28}$$

$$\begin{aligned} h_y = -\mu(\nabla^2\psi)_x + \rho(\psi_y\nabla^2\psi - (\psi_x)_t) - \mu^* f\psi_y(f\nabla^2\psi + f_y\psi_y + f_x\psi_x) \\ -\alpha_1[(\psi_y\nabla^2\psi + (\psi_x)_t)] + \frac{\phi^*}{k}(\mu + \alpha_1\frac{\partial}{\partial t})\psi_x + 2\rho\overrightarrow{\Omega}\psi_y. \end{aligned} \tag{29}$$

Using the integrability condition $h_{xy} = h_{yx}$ and employing (25), (26), (27) in the diffusion equation (21) and solenoidal equation (22), we obtain:

$$\begin{aligned} &\mu\nabla^4\psi - \rho(\nabla^2\psi)_t - (\rho - \mu^* f^2)\frac{\partial(\psi, \nabla^2\psi)}{\partial(x, y)} + \alpha_1\Big[(\nabla^2\psi)_t - \frac{\partial(\psi, \nabla^4\psi)}{\partial(x, y)}\Big] \\ &\quad - \frac{\phi^*}{k}(\mu + \alpha_1\frac{\partial}{\partial t}\nabla^2\psi + 2\rho\Omega(u_y - v_x) \\ &\quad = \mu^*\Big[(\nabla^2\psi + f_x\psi_x + f_y\psi_y)\frac{\partial(\psi, f)}{\partial(x, y)} + f\psi_x\frac{\partial(\psi, f_x)}{\partial(x, y)} + f\psi_y\frac{\partial(\psi, f_y)}{\partial(x, y)} \\ &\quad + ff_x\frac{\partial(\psi, \psi_x)}{\partial(x, y)} + ff_y\frac{\partial(\psi, \psi_y)}{\partial(x, y)}\Big], \end{aligned} \tag{30}$$

$$\mu\nabla^4\psi + 3[f_x(\nabla^2\psi)_x + f_y(\nabla^2\psi)_y] + (\nabla^2 f)(\nabla^2\psi) + (f_{xx}\psi_{xx} + 2f_{xy}\psi_{xy} + f_{yy}\psi_{yy}) + \psi_x(\nabla^2 f)_x + \psi_y(\nabla^2 f)_y = \mu^*\sigma[f(\nabla^2\psi)_t + f_t(\nabla^2\psi) + f_x(\psi_x)_t + f_y(\psi_y)_t + (f_x)_t\psi_x + (f_y)_t\psi_y], \tag{31}$$

$$\frac{\partial(\psi, f)}{\partial(x,y)} = 0. \tag{32}$$

The equation (30) and (31) become

$$\mu\nabla^4\psi - \rho(\nabla^2\psi)_t - (\rho - \mu^* f^2)\frac{\partial(\psi,\nabla^2\psi)}{\partial(x,y)} + \alpha_1\Big[(\nabla^2\psi)_t - \frac{\partial(\psi,\nabla^4\psi)}{\partial(x,y)}\Big] - \frac{\phi^*}{k}(\mu + \alpha_1\frac{\partial}{\partial t}\nabla^2\psi + 2\rho\Omega\omega) = \mu^* f\Big[\psi_x\frac{\partial(\psi, f_x)}{\partial(x,y)} + \psi_y\frac{\partial(\psi, f_y)}{\partial(x,y)} + f_x\frac{\partial(\psi,\psi_x)}{\partial(x,y)} + f_y\frac{\partial(\psi,\psi_y)}{\partial(x,y)}\Big], \tag{33}$$

$$f\nabla^4\psi + 3[f_x(\nabla^2\psi)_x + f_y(\nabla^2\psi)_y] + \nabla^2 f\nabla^2\psi + (f_{xx}\psi_{xx} + 2f_{xy}\psi_{xy} + f_{yy}\psi_{yy}) + \psi_x(\nabla^2 f)_x + \psi_y(\nabla^2 f)_y = \mu^*\sigma[f(\nabla^2\psi)_t + f_t(\nabla^2\psi) + f_x(\psi_x)_t + f_y(\psi_y)_t + (f_x)_t\psi_x + (f_y)_t\psi_y]. \tag{34}$$

Equation (33) and (34) hold true for an unsteady, plane, MHD aligned motion of an rotating incompressible, second grade fluid of finite electriacl conductivity σ. For infinitely conducting flows equation (34) takes the form

$$f(\nabla^2\psi)_t + f_t(\nabla^2\psi) + f_x(\psi_x)_t + f_y(\psi_y)_t + (f_x)_t\psi_x + (f_y)_t\psi_y = 0. \tag{35}$$

3. Exact Solutions

We assume that

$$\nabla^2\psi = y\phi(x), \tag{36}$$

where $\phi(x)$ is an unknown function of its argument.

$$\nabla^4\psi = y\phi''(x). \tag{37}$$

Using equation (36) in equation (33) and for solving analytically we assume that f is a function of t only, we obtain

$$\mu y\phi''(x) - \rho(y\phi''(x))_t + (\rho - \mu^* f^2)(\psi_x\phi''(x) - \psi_y\phi''(x)) + \alpha_1[(y\phi''(x))_t - (\psi_x\phi''(x) - \psi_y\phi''(x))] - \frac{\phi^*}{k}\Big(\mu + \alpha_1\frac{\partial}{\partial t}\Big)y\phi(x) = \mu^* f[({\psi_y}^2 - {\psi_x}^2)f_{xy} + \psi_x\psi_y(f_{xx} - f_{yy}) + (\psi_y\psi_{xx} - \psi_x\psi_{xy})f_x + (\psi_y\psi_{xy} - \psi_x\psi_{yy})f_y] - 2\rho\Omega(u_x - v_y), \tag{38}$$

$$\begin{aligned} fy\phi''(x)+&3[f_x(y\phi(x))_t + f_y\phi(x) + \nabla^2 f(y\phi(x))] + 2(f_{xx}\psi_{xx} + 2f_{xy}\psi_{xy} + f_{yy}\psi_{yy}) \\ &+ \psi_x(\nabla^2 f)_x + \psi_y(\nabla^2 f)_y \\ &= \mu^*[f(\phi(x))_t + f_t y\phi(x) + f_x\psi_{xt} + f_y\psi_{yt} + f_{xt}\psi_x + f_{yt}\psi_y], \end{aligned} \tag{39}$$

$$\begin{aligned} \mu y\phi''(x) - \rho(y\phi''(x))_t + (\rho - \mu^* f^2)(\psi_x\phi(x) - \psi_y\phi'(x)) + \alpha_1[(y\phi''(x))_t \\ -(\psi_x\phi''(x) - \psi_y\phi'''(x))] - \frac{\phi^*}{k}\Big(\mu + \alpha_1\frac{\partial}{\partial t}\Big)y\phi(x) + 2\rho\Omega(u_x - v_y) = 0, \end{aligned} \tag{40}$$

$$\begin{aligned} [(\rho - \mu^* f^2)\phi(x) - \alpha_1\phi''(x)]\frac{\partial\psi}{\partial x} + y[(\rho - \mu^* f^2)\phi'(x) + \alpha_1\phi'''(x)]\frac{\partial\psi}{\partial y} + \mu y\phi''(x) \\ + (\alpha_1 - \rho)(y\phi''(x))_t) - \Big(\frac{\phi^*}{k}\Big(\mu + \alpha_1\frac{\partial}{\partial t}\Big) + 2\rho\Omega\Big)y\phi(x) = 0. \end{aligned} \tag{41}$$

4. For steady flow

We have from (41)

$$\begin{aligned} [(\rho - \mu^* f^2)\phi(x) - \alpha_1\phi''(x)]\frac{\partial\psi}{\partial x} + y[(\rho-\mu^* f^2)\phi'(x) + \alpha_1\phi'''(x)]\frac{\partial\psi}{\partial y} + \mu y\phi''(x) \\ - \Big(\frac{\phi^*}{k}\mu + 2\rho\Omega\Big)y\phi(x) = 0. \end{aligned} \tag{42}$$

4.1. Case I.

4.1. Case I. When

$$(\rho - \mu^* f^2)\phi(x) - \alpha_1\phi''(x) = 0, \tag{43}$$

then integrating (43), we get,

$$\phi(x) = A_1 + A_2 e^{mx} + A_3 e^{-mx}, \tag{44}$$

where

$$m = \sqrt{\frac{\rho - \mu^* f^2}{\alpha_1}}, A_1 \neq 0, A_2, A_3$$

are constants. Then

$$\begin{aligned} \psi(x,y) = -\mu\frac{y\phi'(x)}{(\rho - \mu^* f^2)}y\{A_2 e^{mx} + A_3 e^{-mx}\} \\ - y\Big(\frac{\phi^*}{k}\mu + 2\rho\Omega\Big)\Big(A_1 x + \frac{A_2 e^{mx}}{m} - \frac{A_3 e^{-mx}}{m}\Big) + g(y) \end{aligned} \tag{45}$$

But

$$\psi_{xx} + \psi_{yy} = y\phi(x), \tag{46}$$

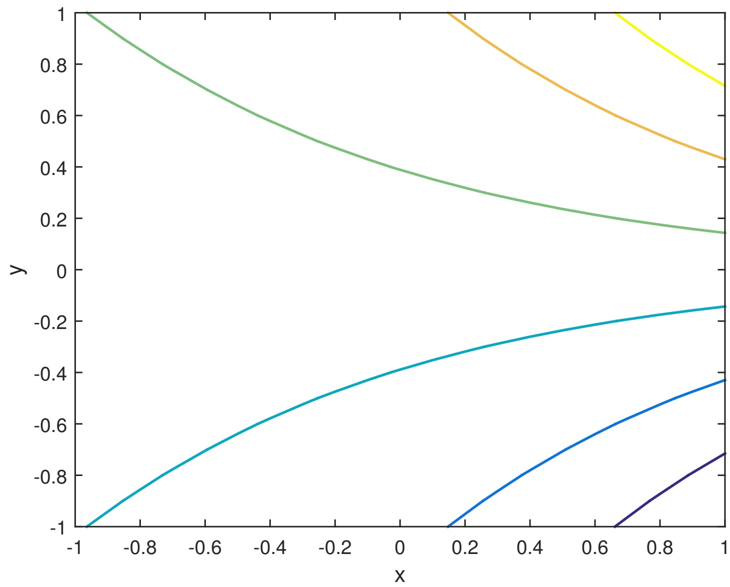

Figure 1: Streamlines profile for $\psi(x,y) = \frac{A_2}{m^2} y e^{mx} - A_1 Bxy + \frac{A_1}{6} y^3 + A_4 y + A_5$, illustrating the combined exponential, cubic, and linear contributions that define the flow structure.

therefore

$$g''(y) = A_1 y + A_2[1 + Am^2 + Bm^2] y e^{mx} + A_3[1 - Am^2 - Bm^2] y e^{-mx} \tag{47}$$

In order for this equation to hold true for all values of x, we must take

$$g''(x) = A_1 y, \;\; A_2[1 + Am^2 + Bm^2] = 0, \;\; A_3[1 + Am^2 + Bm^2] = 0$$

which lead to two subcase. Either

$$(a) \;\; g(y) = \frac{A_1}{6} y^3 + A_4 y + A_5, \;\; A + B = \frac{-1}{m^2}, \;\; A_3 = 0,$$

or

$$(b) \;\; g(y) = \frac{A_1}{6} y^3 + A_4 y + A_5, \;\; A + B = \frac{1}{m^2}, \;\; A_2 = 0,$$

For subcase (a), the stream function as shown in figure 1, the velocity components, vorticity function and the pressure function are given by

$$\psi(x,y) = \frac{A_2}{m^2} y e^{mx} - A_1 Bxy + \frac{A_1}{6} y^3 + A_4 y + A_5,$$

$$u = \frac{A_2}{m^2}e^{mx} - A_1Bx + \frac{A_1}{6}y^2 + A_4,$$
$$v = -\frac{A_2}{m^2}ye^{mx} + A_1Bxy,$$

And velocity of the fluid for steady flow can be shown in figure 2.

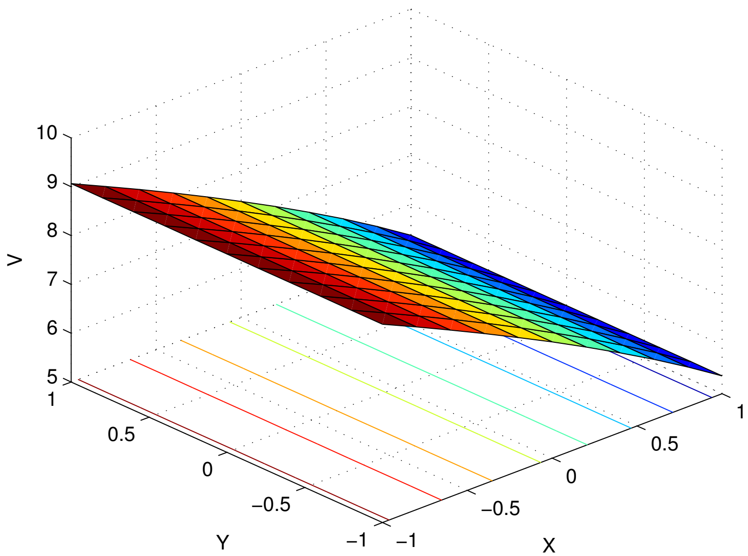

Figure 2: Velocity profile for the steady flow in Case I, highlighting the effect of governing parameters on the distribution.

$$H_1 = f_0\Big\{\frac{A_2}{m^2}e^{mx} - A_1Bx + \frac{A_1}{2}y^2 + A_4\Big\},$$
$$H_2 = -f_0\Big\{\frac{A_2}{m^2}ye^{mx} - A_1Bx - \frac{A_1}{2}y\Big\},$$
$$\omega = -y\{A_1 + A_2e^{mx} + A_3e^{-mx}\}.$$

Also, P can be calculated by putting the value of u, v and h in equation (17).
For subcase (b)

$$\psi(x,y) = \frac{A_3}{m^2}ye^{-mx} - A_1Bxy - \frac{A_1}{6}y^3 + A_4y + A_5,$$
$$u = \frac{A_3}{m^2}e^{-mx} - A_1Bx + \frac{A_1}{6}y^2 + A_4,$$

$$\begin{aligned}
v &= -\frac{A_3}{m^2}ye^{-mx} + A_1Bxy,\\
H_1 &= f_0\Big\{\frac{A_3}{m^2}e^{-mx} - A_1Bx + \frac{A_1}{2}y^2 + A_4\Big\},\\
H_2 &= -f_0\Big\{\frac{A_3}{m^2}ye^{-mx} - A_1Bx - \frac{A_1}{2}y\Big\},\\
\omega &= -y\{A_1 + A_3e^{mx} + A_2e^{-mx}\}.
\end{aligned}$$

Also, P can be calculated by putting the value of u, v and h in equation (17).

4.2. Case II. When

$$(\rho - \mu^* f^2)\phi(x) - \alpha_1\phi''(x) \neq 0 \quad and \quad (\rho - \mu^* f^2)\phi(x) - \alpha_1\phi''(x) \neq 0$$

Letting

$$\gamma = y[(\rho - \mu^* f^2)\phi(x) - \alpha_1\phi''(x)],$$

we find that

$$\frac{\partial(x,\gamma)}{\partial(x,y)} = (\rho - \mu^* f^2)\phi(x) - \alpha_1\phi''(x) \neq 0.$$

Now equation (42) can be transform into new independent variables x, γ and integrating with respect to x, we have

$$\psi(x,\gamma) = -\mu\gamma\int\frac{(\phi''(x) + \frac{\phi^*}{k}\mu + 2\rho\Omega\phi(x) + N)}{(\beta\phi(x) - \alpha_1\phi''(x))^2}dx + \theta(\gamma), \tag{48}$$

where $\theta(\gamma)$ is arbitrary function of γ and $\beta = (\rho - \mu^* f^2)$. Using (48) in (36), we obtain

$$\begin{aligned}
&-\mu\gamma\frac{(\beta\phi''(x) - \alpha_1\phi^{iv}(x))}{(\beta\phi(x) - \alpha_1\phi''(x))}\int\frac{(\phi''(x) + \frac{\phi^*}{k}\mu + 2\rho\Omega\phi(x) + N)}{(\beta\phi(x) - \alpha_1\phi''(x))^2}dx\\
&+\gamma\theta'(\gamma)\frac{(\beta\phi''(x) - \alpha_1\phi^{iv}(x))}{\beta\phi(x) - \alpha_1\phi''(x)} + \gamma^2\theta''(\gamma)\frac{(\beta\phi''(x) - \alpha_1\phi^{iv}(x))^2}{(\beta\phi(x) - \alpha_1\phi''(x))^2}\\
&-\mu\gamma\frac{(\phi'''(x) - 2\rho\Omega\phi'(x))^2}{(\beta\phi(x) - \alpha_1\phi''(x))^2} + (\beta\phi(x) - \alpha_1\phi''(x))^2\theta''(\gamma) - \frac{\gamma\phi}{\beta\phi(x) - \alpha_1\phi''(x)} = 0.
\end{aligned} \tag{49}$$

Differentiating equation (49) twice with respect to γ, we have

$$\begin{aligned}
&[\gamma\theta'(\gamma)]''\frac{(\beta\phi''(x) - \alpha_1\phi^{iv}(x))}{(\beta\phi(x) - \alpha_1\phi''(x))} + [\gamma^2\theta''(\gamma)]''\frac{(\beta\phi''(x) - \alpha_1\phi^{iv}(x))^2}{(\beta\phi(x) - \alpha_1\phi''(x))^2}\\
&\qquad + (\beta\phi(x) - \alpha_1\phi''(x))^2\theta^{iv}(\gamma) = 0.
\end{aligned} \tag{50}$$

Dividing equation (50) by $(\beta\phi(x) - \alpha_1\phi''(x))^2 \neq 0$ and differentiating with respect to x, we obtain

$$[\gamma\theta'(\gamma)]''\left\{\frac{(\beta\phi''(x) - \alpha_1\phi^{iv}(x))}{(\beta\phi(x) - \alpha_1\phi''(x))^3}\right\}' + [\gamma^2\theta''(\gamma)]''\left\{\frac{(\beta\phi''(x) - \alpha_1\phi^{iv}(x))^2}{(\beta\phi(x) - \alpha_1\phi''(x))^4}\right\}' = 0 \quad (51)$$

The following subcases arises

$$(a)\quad [\gamma\theta'(\gamma)]'' = [\gamma^2\theta''(\gamma)]'' = 0,$$

$$(b)\quad \left\{\frac{(\beta\phi''(x) - \alpha_1\phi^{iv}(x))}{(\beta\phi(x) - \alpha_1\phi''(x))^3}\right\}' = \left\{\frac{(\beta\phi'(x) - \alpha_1\phi^{iii}(x))^2}{(\beta\phi(x) - \alpha_1\phi''(x))^4}\right\}' = 0,$$

$$(c)\quad [\gamma\theta'(\gamma)]'' = \left\{\frac{(\beta\phi'(x) - \alpha_1\phi^{iii}(x))^2}{(\beta\phi(x) - \alpha_1\phi''(x))^4}\right\}' = 0,$$

$$(d)\quad [\gamma^2\theta''(\gamma)]'' = \left\{\frac{(\beta\phi''(x) - \alpha_1\phi^{iv}(x))}{(\beta\phi(x) - \alpha_1\phi''(x))^3}\right\}' = 0,$$

$$(e)\quad [\gamma\theta'(\gamma)]'' \neq 0 and \left\{\frac{(\beta\phi'(x) - \alpha_1\phi^{iii}(x))^2}{(\beta\phi(x) - \alpha_1\phi''(x))^4}\right\}' \neq 0.$$

Subcases (b) to (e) lead to contradictions. We consider subcase (a) in the following subcase

$$(a)\quad [\gamma\theta'(\gamma)]'' = [\gamma^2\theta''(\gamma)]'' = 0.$$

Integrating $[\gamma\theta'(\gamma)]'' = 0$ three times with respect to γ, we obtain

$$\theta(\gamma) = a\gamma + blogr + c \quad (52)$$

where a, b, c are constant of integration. using (52), equation $[\gamma^2\theta''(\gamma)]'' = 0$ is identically satisfied and equation (51) gives us b = 0. Using (52) with b = 0 in equation (49), we get

$$\begin{aligned} &-\mu\frac{(\beta\phi''(x) - \alpha_1\phi^{iv}(x))}{(\beta\phi(x) - \alpha_1\phi''(x))}\int\frac{(\phi''(x) + 2\rho\Omega\phi(x) + N)}{(\beta\phi(x) - \alpha_1\phi''(x))}dx \\ &+ a\frac{(\beta\phi''(x) - \alpha_1\phi^{iv}(x))}{(\beta\phi(x) - \alpha_1\phi''(x))} - \mu\frac{(\phi'''(x) - 2\rho\Omega\phi'(x))}{(\beta\phi(x) - \alpha_1\phi''(x))^2} - \frac{\phi(x)}{(\beta\phi(x) - \alpha_1\phi''(x))} = 0. \end{aligned} \quad (53)$$

Then the stream function is given by

$$\begin{aligned} \psi(x, y) = -\mu y(\beta\phi(x) - \alpha_1\phi''(x))&\int\frac{(\phi''(x) + 2\rho\Omega\phi(x) + N)}{(\beta\phi(x) - \alpha_1\phi''(x))^2}dx \\ &+y(\beta\phi(x) - \alpha_1\phi''(x)) + c. \end{aligned} \quad (54)$$

where the function $\phi(x)$ satisfies equation (53). For example, let $\phi(x) = e^{kx}$ such that $k \neq \pm\sqrt{\frac{\rho}{\alpha_1}}$. Then equation (53) implies that $a = \frac{1}{k^2(\beta-\alpha_1 k^2)}\left[1 - \frac{\mu k N e^{-2kx}}{(\beta-\alpha_1 k^2)}\right]$. For this special case, the stream function is given by

$$\psi(x,y) = -\mu(k^2 + 2\rho\Omega)xy + \mu N k y e^{kx} + ay(\beta - \alpha_1 k^2)e^{kx} + c.$$

5. For unsteady flow

For unsteady flow solving equation (41), we have

$$\psi = \frac{-1}{m^2+n^2}[G_1 cos(nx - my) + G_2 sin(nx + my)]e^{\frac{-Ft}{\mu^*\sigma}}, \tag{55}$$

The streamlines are hyperbolic can be shown in the figure 3.

$$u = m\frac{-1}{m^2+n^2}[-G_1 sin(nx - my) + G_2 cos(nx + my)]e^{\frac{-Ft}{\mu^*\sigma}}, \tag{56}$$

$$v = n\frac{-1}{m^2+n^2}[-G_1 sin(nx - my) + G_2 cos(nx + my)]e^{\frac{-Ft}{\mu^*\sigma}}, \tag{57}$$

$$H_1 = f_0 m\frac{-1}{m^2+n^2}[G_1 sin(nx - my) + G_2 cos(nx + my)]e^{\frac{-Ft}{\mu^*\sigma}}, \tag{58}$$

$$H_2 = -f_0 n\frac{-1}{m^2+n^2}[G_1 sin(nx - my) + G_2 cos(nx + my)]e^{\frac{-Ft}{\mu^*\sigma}}, \tag{59}$$

$$\omega = F[G_1 cos(nx - my) + G_2 sin(nx + my)]e^{\frac{-Ft}{\mu^*\sigma}}, \tag{60}$$

$$J = -f_0 F[G_1 cos(nx - my) + G_2 sin(nx + my)]e^{\frac{-Ft}{\mu^*\sigma}}. \tag{61}$$

Also, P can be calculated by putting the value of u, v and h in equation (17).

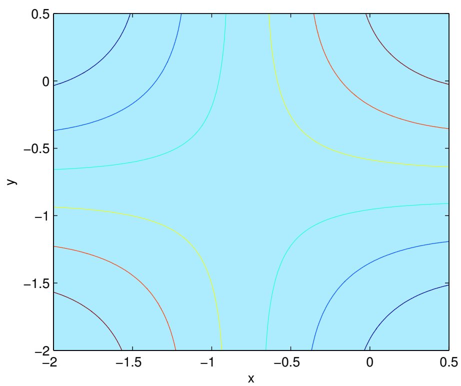

Figure 3: Streamlines for the unsteady flow case, showing instantaneous patterns derived from the stream function.

6. Exact solution for $\psi(x,y) = g(x) + h(y)$

We assume that the stream function $\psi(x,y)$ is of the form

$$\psi(x,y) = g(x) + h(y) : \quad g'(x) \neq 0, h'(x) \neq 0 \tag{62}$$

where $f(x)$ and $g(y)$ are arbitrary functions. Substituting (62) in (31), we obtain

$$g'[(\rho-\mu^* f^2)h''' - \alpha_1 h^v] + h'[\alpha_1 g^v - (\rho-\mu^* f^2)g'''] + \mu(g^{iv} + h^{iv}) + \frac{\phi^*}{k}\mu(g''+h'') - 2\rho\Omega\omega = 0 \tag{63}$$

$$g''[(\rho - \mu^* f^2)h^{iv} - \alpha h^{iv}] - h''[(\rho - \mu^* f^2)g^{iv} - \alpha g^{vi}] = 0. \tag{64}$$

6.1. Case I. When

$$g'' = 0, h'' = 0. \tag{65}$$

In this case, the functions $g(x)$ and $h(y)$ are given by $g(x) = a_0 + a_1 x$ and $h(y) = a_2 y$, where a_0, a_1 and a_2 are arbitrary constants. Thus, the stream function can be shown in the figure 4, the velocity component and the pressure function are given by

$$\psi(x,y) = a_0 + a_1 x + a_2 y, u(x,y) = a_2, v(x,y) = -a_1, \tag{66}$$

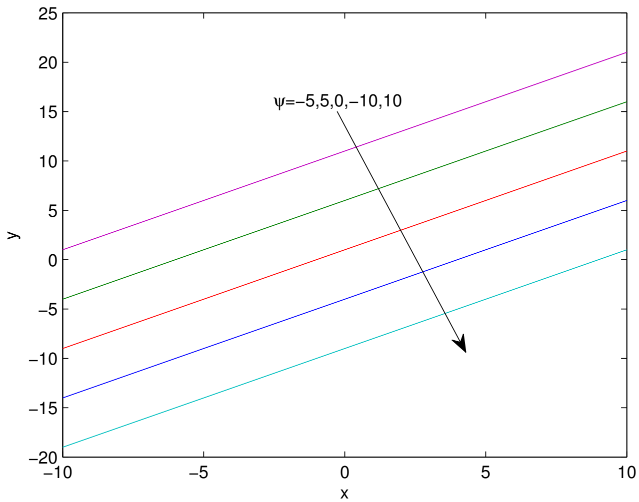

Figure 4: Streamline profile for steady flow of section 6.1 case I $\psi(x,y) = a_0 + a_1 x + a_2 y$, illustrating a uniform flow with straight parallel paths.

Figure 4 illustrates uniform, parallel streamlines, indicating a simple shear flow where rotation and magnetic effects do not distort the basic flow structure.

$$H_1 = f a_2, H_2 = -f a_1, \tag{67}$$

$$P(x,y,t) = \big(\frac{\phi^*}{k} - 2\rho\Omega\big)(a_2x - a_1y) - \frac{1}{2}\rho({a_2}^2 + {a_1}^2) + P_0. \quad (68)$$

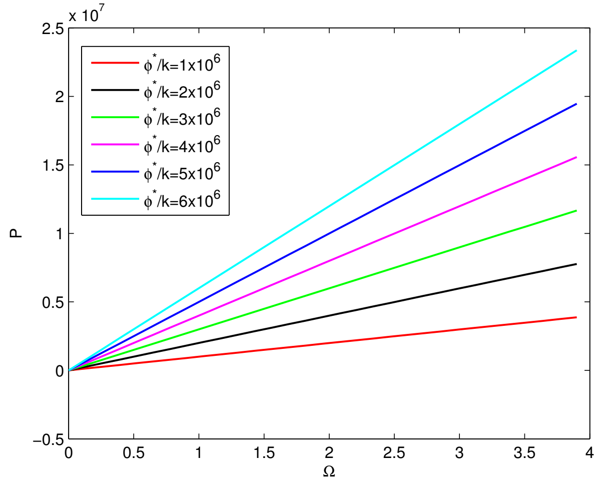

Figure 5: Pressure variation with angular velocity at constant density ρ for different values of the $\frac{\phi^*}{k}$ ranging from 1×10^6 to 6×10^6, illustrating how increasing $\frac{\phi^*}{k}$ shifts the pressure response.

Figure 5 shows that fluid pressure increases linearly with angular velocity, demonstrating that higher porosity resistance amplifies rotational effects in the porous medium.

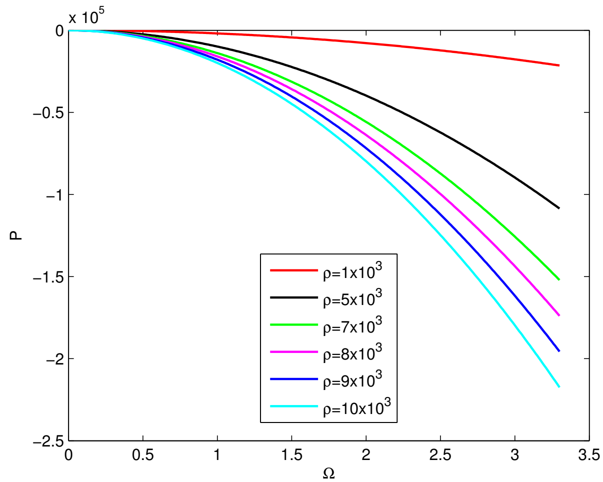

Figure 6: Fluid pressure variation with angular velocity for progressively increasing densities, showing the nonlinear dependence of pressure response on rotational motion.

Figure 6 indicates that increasing fluid density reduces pressure with angular velocity, highlighting the dominant inertial effects of denser fluids in a rotating frame.
6.2. Case II. When

$$g'' = 0, h'' \neq 0. \tag{69}$$

In this case, the equation (64) is identically satisfied and the equation (63) becomes

$$b_0[(\rho - \mu^* f^2)h^{iii} - \alpha h^v] + \mu h^{iv}(y) = 0, b_0 = g'(x) \neq 0 \tag{70}$$

with general solution given by

$$h(y) = b_1 + b_2 y + b_3 y^2 + b_4 e^{m_1 y} + b_5 e^{m_2 y}, \quad m_{1,2} = \frac{\mu \pm \sqrt{\mu^2 + 4\alpha_1(\rho - \mu^* f^2)b_0}}{2\alpha_1 b_0} \tag{71}$$

where$b_0 \neq 0$, b_1, b_2, b_3, b_4 and b_5 are arbitrary constants. Thus, the stream function, the velocity components and the pressure function for, this case, are given by

$$\psi(x, y) = b_0 x + b_1 + b_2 y + b_3 y^2 + b_4 e^{m_1 y} + b_5 e^{m_2 y}, \tag{72}$$

The streamline pattern is shown in figure 7.

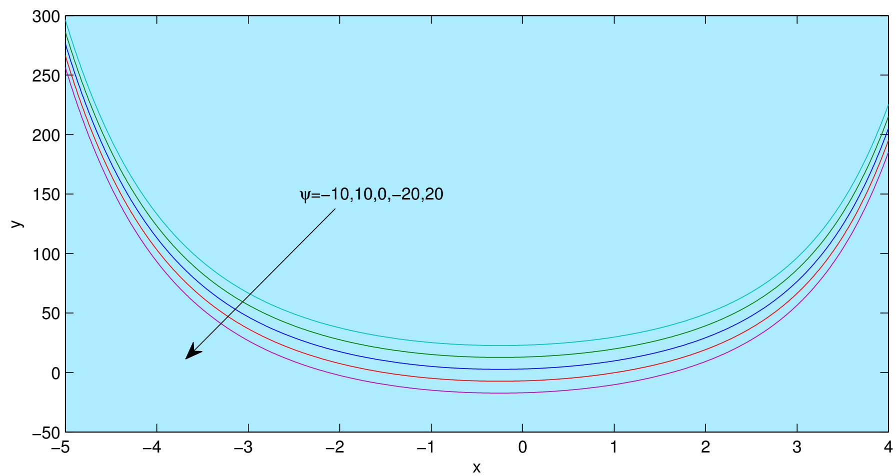

Figure 7: Streamline profiles for unsteady flow (Case II) showing how the flow grows and decays along the x direction due to the parabolic and exponential terms together.

Figure 7 presents curved streamlines, reflecting the combined influence of rotation and non-Newtonian effects on flow deflection.

$$u(x, y) = b_2 + 2b_3 y + m_1 b_4 e^{m_1 y} + m_2 b_5 e^{m_2 y}, \quad v = -b_0, \tag{73}$$

$$P = (\frac{\phi^*}{k} - 2\rho\Omega)((b_2 + 2b_3y + m_1b_4e^{m_1y} + m_2b_5e^{m_2y})x - b_0y) \\ +\frac{\rho}{2}((b_2 + 2b_3y + m_1b_4e^{m_1y} + m_2b_5e^{m_2y})^2 + b_0) + P_0. \tag{74}$$

where P_0 is an arbitrary constant of integration.

6.3. Case III. When

$$g'' \neq 0, h'' = 0 \tag{75}$$

Proceeding as in case II, we obtain

$$\begin{aligned} &\psi(x,y) = c_1 + c_2x + (c_3 + c_4x)e^{-m_1x} + c_5e^{m_2x} + c_6y, \\ &u(x,y) = c_6, v(x,y) = c_2 + c_3e^{-m_1x} + c_4(x-1)e^{-m_1x} + c_5e^{-m_2x}, \\ &P(x,y) = -\rho c_6\{c_4(1+2x)e^{-m_1x} + c_5e^{m_1x}\}y + \mu\{2c_4e^{-m_1x} + c_5e^{m_1x}\}y \\ &\quad + \alpha_1[\{2c_5e^{m_1x} - 2(3c_4 + c_3)e^{-m_1x}\}y + (c_5e^{m_2x} - c_3e^{-m_1x})] \\ &\quad + \alpha_2[\{c_5e^{m_1x} - (3c_4 + c_3)e^{-m_1x}\}y + \{c_5e^{m_2x} - (c_4' + c_4(1+x))e^{-m_1x}\}] \\ &\quad + (\frac{\phi^*}{k}\mu + 2\rho\Omega)\{(c_3 + c_4(1+x))e^{-m_1x} + c_5e^{m_2x} + c_6^2x\} \\ &\quad - \frac{1}{2}\{[c_2 + c_4(1-x)c_3e^{-m_1x} + c_5e^{m_2x}]^2 + c_6^2\}. \end{aligned} \tag{76}$$

6.4. Case IV. When

$$g'' \neq 0, h'' \neq 0. \tag{77}$$

Dividing equation (64) by $g''(x)h''(y) \neq 0$, we obtain

$$\frac{(\rho - \mu^*f^2)h^{iv}(y) - \alpha_1h^{vi}(y)}{h''(y)} - \frac{(\rho - \mu^*f^2)g^{iv}(x) - \alpha_1g^{vi}(x)}{g''(x)} = 0. \tag{78}$$

Equation (78) implies that

$$\frac{(\rho - \mu^*f^2)g^{iv}(x) - \alpha_1g^{vi}(x)}{g''(x)} - \lambda g''(x) = 0, \tag{79}$$

$$\frac{(\rho - \mu^*f^2)h^{iv}(y) - \alpha_1h^{vi}(y)}{h''(y)} - \lambda h''(y) = 0, \tag{80}$$

where λ is an arbitrary constant. We let the solution of equation (79) to be of the form $g(x) = e^{mx}$, where m is given by

$$m^2(\alpha_1m^4 - (\rho - \mu^*f^2)m^2 + \lambda) = 0. \tag{81}$$

The roots of this equation are

$$m = 0 \quad and \quad m^2 = \frac{(\rho - \mu^* f^2) \pm \sqrt{(\rho - \mu^* f^2)^2 - 4\alpha_1 \lambda}}{2\alpha_1}. \tag{82}$$

Four possibilities arises: (a) $\lambda = 0$, (b) $\lambda = (\rho - \mu^* f^2)^2$, (c) $(\rho - \mu^* f^2)^2 - 4\alpha_1\lambda > 0$ and (d) $(\rho - \mu^* f^2)^2 - 4\alpha_1\lambda < 0$. Possibility (d) leads to a contradiction.

6.4.1. Possibility (a): $\lambda = 0$

In this case, the general solutions of equations (79) and (80) are given by

$$\begin{aligned} g(x) &= B_0 + B_1 x + B_2 x^2 + B_3 x^3 + B_4 e^{mx} + B_5 e^{-mx}, \\ h(y) &= C_0 + C_1 y + C_2 y^2 + C_3 y^3 + C_4 e^{my} + C_5 e^{-my}, \end{aligned} \tag{83}$$

where $m = \sqrt{\frac{\rho - \mu^* f^2}{\alpha_1}}$ and $B_1, C_i, i = 0, 1, ..5$ are constants. Using equations (83) in (63), we find that either

(1)$B_3 = B_4 = B_5 = C_3 = C_4 = C_5 = 0$,

(2)$B_1 = B_2 = B_3 = B_4 = C_4 = C_5 = 0,\ C_3 = \mu \frac{m^3}{6(\rho - \mu^* f^2)}$,

(3)$B_1 = B_2 = B_3 = B_5 = C_4 = C_5 = 0,\ C_3 = -\mu \frac{m^3}{6(\rho - \mu^* f^2)}$,

(4)$B_4 = B_5 = C_1 = C_2 = C_3 = C_4 = 0,\ B_3 = -\mu \frac{m^3}{6(\rho - \mu^* f^2)}$,

(4)$B_4 = B_5 = C_1 = C_2 = C_3 = C_5 = 0,\ B_3 = \mu \frac{m^3}{6(\rho - \mu^* f^2)}$.

The stream function, velocity components and the pressure for each one of these five cases are given by:

for (1):

$\psi(x, y) = B_0 + B_1 x + B_2 x^2 + C_0 + C_1 y + C_2 y^2,\ u(x, y) = C_1 + 2C_2 y,\ v(x, y) = -(B_1 + 2B_2 x)$,

$$\begin{aligned} P = 2\rho\{C_2(B_1 x + 2B_2 x^2) - B_2(C_1 y + C_2 y^2) y\} \\ + \frac{\phi^*}{k}(\mu + 2\rho\Omega)[(B_1 y + 2B_2 xy) - (C_1 x + 2C_2 xy)] \\ - \frac{1}{2}\rho[(C_1 + 2C_2 y)^2 + (B_1 + 2B_2 x)^2] + P_0. \end{aligned} \tag{84}$$

for (2):

$\psi(x, y) = B_0 + B_5 e^{-mx} + C_0 + C_1 y + C_2 y^2 + \frac{\mu m^3}{6\rho} y^3,\ u = C_1 + 2C_2 y + \frac{\mu m^3}{6\rho} y^3$, $v = m B_5 e^{-mx}$,

$$P = \rho B_5 e^{mx} \Big\{ 2C_2 + \Big(\frac{\mu m^3}{\rho} + 1 \Big) y + C_2 y^2 + \frac{\mu m^3}{6\rho} y^3 \Big\}$$

$$
\begin{aligned}
&+\frac{\mu m^3}{\rho}x + m^3 B_5 e^{-mx}\{(\mu-\alpha_1 m+2\alpha_2)y-2\alpha_2\}\\
&-\frac{\phi^*}{k}(\mu+2\rho\Omega)\Big\{C_1+(2C_2+mB_5e^{-mx})y+\frac{\mu m^3}{6\rho}xy^2\Big\}\\
&-\frac{1}{2}\Big[\Big(C_1+2C_2y+\frac{\mu m^3}{6\rho}y^3\Big)^2+(mB_5e^{-mx})^2\Big]+P_0.
\end{aligned} \tag{85}
$$

for (3):

$\psi(x,y) = B_0 + B_4e^{mx} + C_0 + C_1y + C_2y^2 - \frac{\mu m^3}{6\rho}y^3$, $u = C_1 + 2C_2y + \frac{\mu m^3}{2\rho}y^2$, $v = -mB_5e^{mx}$,

$$
\begin{aligned}
P = {} & \rho B_4 e^{mx}\Big\{m^2\Big(C_1y+C_2y^2-\frac{\mu m^3}{6\rho}y^3\Big)+2C_2-\frac{\mu m^3}{\rho}y\Big\}-\frac{\mu m^3}{6\rho}x\\
&-m^2B_4e^{mx}\Big\{2\alpha(1+my)-\alpha_1\Big(C_1y+C_2y^2-\frac{\mu m^3}{6\rho}y^3\Big)\Big\}\\
&+\frac{\phi^*}{k}(\mu+2\rho\Omega)\Big[mB_4e^{mx}y-\Big(C_1+2C_2y-\frac{\mu m^3}{6\rho}y^2\Big)x\Big]-\\
&\frac{1}{2}\rho\Big[\Big(C_1+2C_2y+\frac{\mu m^3}{6\rho}y^3\Big)^2+(mB_5e^{mx})^2\Big]+P_0.
\end{aligned} \tag{86}
$$

for (4):

$\psi(x,y) = B_0 + B_1x + B_2 - \frac{\mu m^3}{6\rho}x^3 + C_0 + C_1e^{-my}$, $u = -mC_5e^{-my}$, $v = -\Big(B_1x + B_2 - \frac{\mu m^3}{2\rho}x^2\Big)$,

$$
\begin{aligned}
P = {} & \rho\Big[m^2C_5e^{-my}\Big(B_1x+B_2x^2-\frac{\mu m^3}{6\rho}x^3\Big)+\frac{\mu m^3}{\rho}x-2B_2\Big(B_1+2B_2x-\frac{\mu m^3}{2\rho}x^2\Big)y\Big]\\
&-\frac{\mu^2m^3}{6\rho}y-\mu m^2C_5e^{-my}x-\alpha_1\Big\{\Big(2B_2-\frac{\mu m^3}{\rho}x\Big)(-m^2C_5e^{-my})\Big\}-2\mu m^3\alpha_2(x+y)\\
&+\frac{\phi^*}{k}(\mu+2\rho\Omega)\Big\{mC_5e^{-my}x+\Big(B_1+2B_2x-\frac{\mu m^3}{2\rho}x^2\Big)y\Big\}-(mC_5e^{-my})^2\\
&+((B_1x+B_2-\frac{\mu m^3}{2\rho}x^2)^2]+P_0.
\end{aligned} \tag{87}
$$

for (5):

$\psi(x,y) = B_0 + B_1x + B_2 - \frac{\mu m^3}{6\rho}x^3 + C_0 + C_1e^{my}$, $u = mC_5e^{my}$, $v = -\Big(B_1x + B_2 -$

$\frac{\mu m^3}{2\rho}x^2\Big)$,

$$P = \rho C_5 e^{my}\Big[m^2\Big(B_1 x + B_2 - \frac{\mu m^3}{2\rho}x^3\Big) + \Big(2B_2 + \frac{\mu m^3}{\rho}x\Big)\Big] + \mu m^3 C_5 e^{my} x - \frac{\mu m^3}{\rho}(4\alpha_2 + \alpha_1 + 1)y + \frac{\phi^*}{k}(\mu + 2\rho\Omega)\Big[B_1 x + B_2 x^2 + \frac{\mu m^3}{2\rho}x^3 + \Big(B_1 x + B_2 x^2 + \frac{\mu m^3}{2\rho}x^2\Big)y\Big] - \frac{1}{2}\rho\Big[(mC_5 e^{my})^2 + \Big(B_1 x + B_2 - \frac{\mu m^3}{2\rho}x^2\Big)^2\Big] + P_0. \tag{88}$$

where P_0 is an arbitrary constant of integration.

6.4.2. Possibility (b): $\lambda = \frac{(\rho - \mu^* f^2)^2}{4\alpha_1}$

In this case, the general solution of equations (79) and (80) are given by

$$f(x) = D_0 + D_1 x + D_2 e^{mx} + D_3 e^{-mx}, \quad g(y) = E_0 + E_1 y + E_2 + E_2 e^{my} + E_3 e^{-my}, \tag{89}$$

where $m = \sqrt{\frac{(\rho - \mu^* f^2)^2}{4\alpha_1}}$ and $D_1, E_1, i = 0, 1, 2, 3$ are arbitrary constants. Using (89) in equation (63), we find that either
(1)$D_2 = E_2 = 0,\ D_1 = \frac{\mu m^3}{\rho}x^2,\ E_1 = 2\frac{\mu m^3}{\rho}$, or (2)$D_3 = E_2 = 0,\ D_1 = E_1 = \frac{2\mu m^3}{\rho}$
(3)$D_2 = E_3 = 0,\ D_1 = E_1 = -\frac{\mu m^3}{\rho}$ or (4)$D_3 = E_1 = 0,\ D_1 = -\frac{\mu m^3}{\rho},\ E_1 = \frac{\mu m^3}{\rho}$

The stream function the velocity components and the pressure for the each one of these four cases are given by

for (1):

$\psi(x, y) = D_0 + \frac{\mu m^3}{\rho}(x - y) + D_3 e^{-mx} + E_0 + E_3 e^{-my}$,
$u = -\frac{2\mu m}{\rho} - E_3 m e^{-my},\ v = -\frac{2\mu m}{\rho} - D_3 m e^{-mx}$,

$$P = \rho m^2 e^{-mx}\Big\{E_3 m\Big(\frac{2\mu x m}{\rho} + D_3 e^{mx}\Big) + \Big(e^{-my} - \frac{2\mu m}{\rho}y\Big)\Big\} + \mu_1 m^3 e^{-my}(D_3 y - E_3 x) + \alpha_1 D_3\Big[\frac{2\mu m^5}{\rho}(x - e^{-mx}y) + m^3 e^{-mx}(E_3 m^2 x + y) + E_3 m^4 e^{-m(x+y)} - m^4 e^{-mx}(\frac{2\mu}{\rho} - 1)\Big] - 2\alpha_2 D_3 m e^{-mx}(1 + my) + \frac{\phi^*}{k}(\mu - 2\rho\Omega)\Big[2\frac{\mu m}{\rho}(x - y) - E_3 e^{-my}x - 2\frac{\mu m}{\rho} + D_3 e^{mx}y)\Big] - \frac{1}{2}\rho\Big[\Big(-\frac{2\mu m}{\rho} - E_1 m e^{-my}\Big)^2 + \Big(-\frac{2\mu m}{\rho} - D_3 m e^{-mx}\Big)^2\Big] + P_0. \tag{90}$$

for (2):
$\psi(x,y) = D_0 + \frac{\mu m^3}{\rho}(x+y) + D_3e^{mx} + E_0 + E_3e^{-my}$,
$u = \frac{2\mu m}{\rho} - E_3me^{-my}$, $v = -\frac{2\mu m}{\rho} - D_3me^{-mx}$,

$$\begin{aligned} P &= -2\rho D_3E_3m^2e^{m(x-y)} + 2E_3\mu m^3(xe^{-my} - ye^{mx}) + \mu m^3(E_3e^{-my}x - D_3e^{mx}y) \\ &+ \alpha_1\Big[\frac{\mu m^3}{2\rho}(y - E_3m^5e^{-my}x) + D_3E_3m^4e^{m(x-y)}2D_3E_3m^5e^{mx} + D_3E_3m^4e^{m(x-y)}\Big] \\ &+ 2\alpha_2D_3m^2e^{mx}(1+my) \\ &- \frac{\phi^*}{k}(\mu + 2\rho\Omega)\Big[2\frac{\mu m}{\rho}(x+y) - m(E_3e^{-my}x + D_3e^{my}y)\Big] \\ &- \frac{1}{2}\rho\Big[\Big(-\frac{2\mu m}{\rho} - E_1me^{-my}\Big)^2 + \Big(\frac{2\mu m}{\rho} - D_3me^{-mx}\Big)^2\Big] + P_0. \end{aligned} \tag{91}$$

for (3):
$\psi(x,y) = D_0 + \frac{\mu m^3}{\rho}(x+y) + D_3e^{mx} + E_0 + E_2e^{my}$,
$u = -\frac{2\mu m}{\rho} + E_2me^{my}$, $v = \frac{2\mu m}{\rho} + D_3me^{-mx}$,

$$\begin{aligned} P &= -2\rho D_3E_2m^2e^{m(y-x)} + 2\mu m^3(E_3e^{my} - e{-}mx) + D_3\mu m^2e^{-mx}(1+my) \\ &+ \alpha_1\frac{2\mu}{\rho}m^5e^{my}(x+y) + 2\alpha_2D_3m^2e^{-mx}(x-y) \\ &- \frac{\phi^*}{k}(\mu - 2\rho\Omega)\Big[\frac{2\mu m}{\rho}(y-x) + D_2me^{-mx}y + E_2me^{my}x\Big] \\ &- \frac{1}{2}\rho\Big[\Big(-\frac{2\mu m}{\rho} + E_2me^{-my}\Big)^2 + \Big(\frac{2\mu m}{\rho} + D_3me^{-mx}\Big)^2\Big] + P_0. \end{aligned} \tag{92}$$

for (4):
$\psi(x,y) = D_0 + \frac{\mu m^3}{\rho}(y-x) + D_2e^{-mx} + E_0 + E_2e^{my}$,
$u = \frac{2\mu m}{\rho} + E_2me^{my}$, $v = \frac{2\mu m}{\rho} - D_2me^{mx}$,

$$\begin{aligned} P &= 2\rho D_2E_2m^2e^{m(x+y)} - 2\mu m^3xe^{my} + 2D_2m^3xe^{my} + \mu m^3e^{my}(E_2x - D_2y) \\ &+ \alpha_1\Big[\frac{2\mu m^5}{\rho}E_2e^{my}(x+1)\Big] - 4\alpha_2D_2m^3e^{mx} \\ &- \frac{\phi^*}{k}(\mu - 2\rho\Omega)\Big[\frac{2\mu m}{\rho}(x+y) + (E_2e^{my}x + D_2e^{my}y)\Big] \\ &- \frac{1}{2}\rho\Big[\Big(\frac{2\mu m}{\rho} + E_2me^{my}\Big)^2 + \Big(\frac{2\mu m}{\rho} - D_2me^{mx}\Big)^2\Big] + P_0. \end{aligned} \tag{93}$$

where P_0 is an arbitrary constant of integration.

6.4.3. Possibility (c): $(\rho - \mu^* f^2)^2 - 4\alpha_1\lambda > 0$

Since $(\rho - \mu^* f^2) + \sqrt{(\rho - \mu^* f^2)^2 - 4\alpha_1\lambda} > 0$, and $(\rho - \mu^* f^2) - \sqrt{(\rho - \mu^* f^2)^2 - 4\alpha_1\lambda} > 0$, then the solutions of equation (79) and (80) are given by

$$\begin{aligned} g(x) &= A_0 + A_1 x + A_2 e^{m_1 x} + A_3 e^{-m_1 x} + A_4 e^{m_2 x} + A_5 e^{-m_2 x}, \\ h(y) &= B_0 + B_1 y + B_2 e^{m_1 x} + B_3 e^{-m_1 x} + B_4 e^{m_2 x} + B_5 e^{-m_2 x} \end{aligned} \tag{94}$$

where $m_{1,2} = \frac{1}{\sqrt{2\alpha_1}}\sqrt{(\rho - \mu^* f^2) - \pm\sqrt{(\rho - \mu^* f^2)^2 - 4\alpha_1\lambda}}$ and $A_i, B_i, i = 01, 2.., 5$ are arbitray constants. Employing (94) in equation (63), we find that the only possible solutions of the resulting equation has been studied by Siddiqui and Kaloni.

The different streamline patterns can be shown in the figures 8 and 9, velocity profiles (figures 10 and 11) and pressure are shown in following figures.

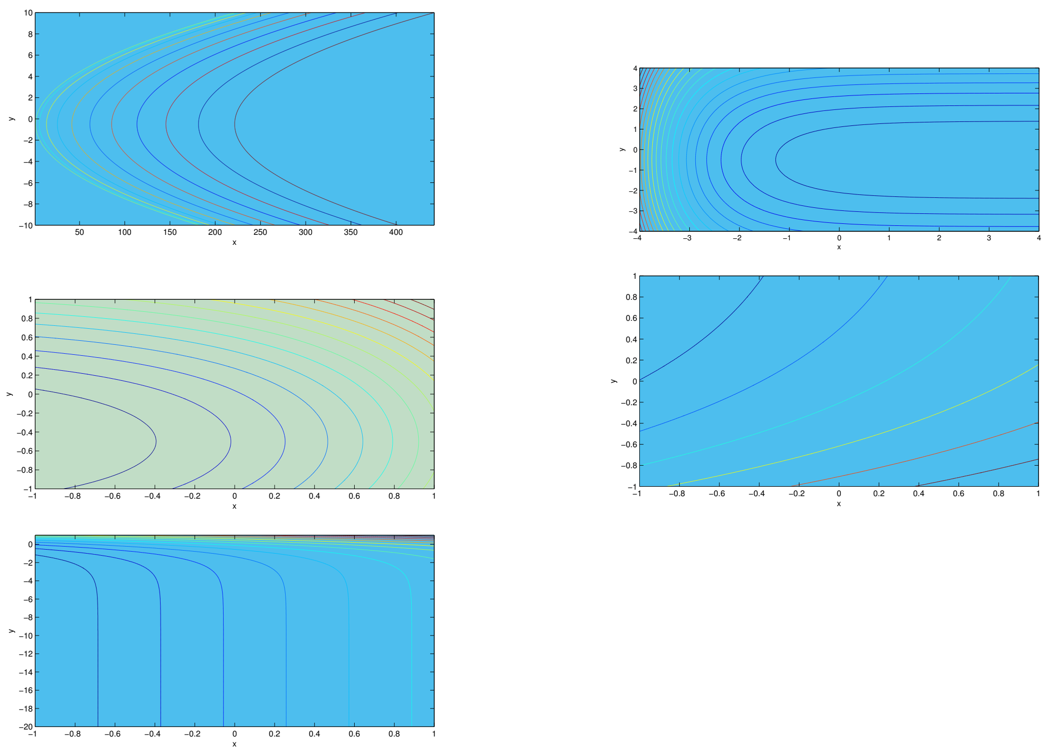

Figure 8: Streamline profiles for $\psi(x, y) = g(x) + h(y)$ in case 6.4 with $\lambda = 0$, illustrating the symmetric flow structure arising from the independent contributions of $g(x)$ and $h(y)$.

Figure 8 shows symmetric streamline patterns, indicating a balanced interaction between rotation and magnetic forces when the parameter λ vanishes.

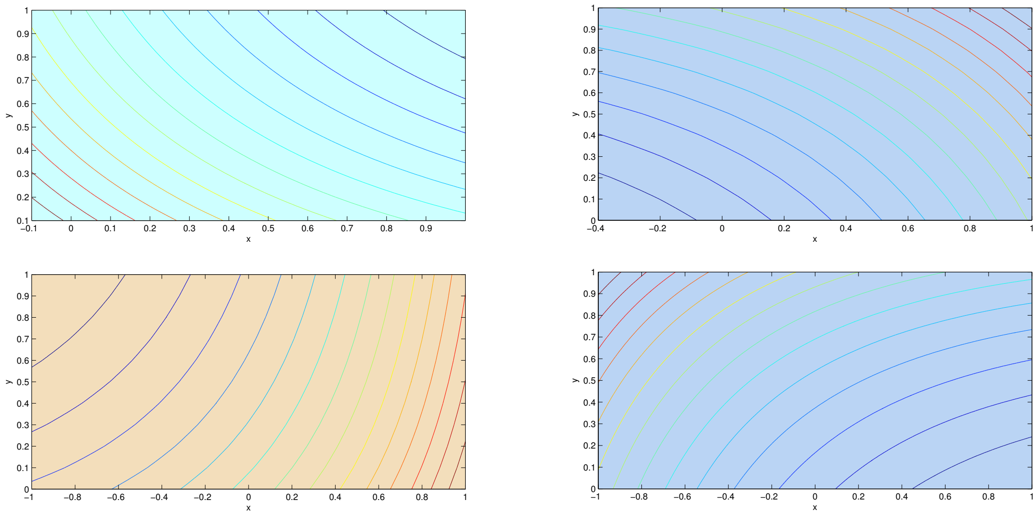

Figure 9: Streamline profiles for $\psi(x, y) = g(x)+h(y)$ in case 6.4 with $\lambda = \frac{\rho-\mu f^2)^2}{4\alpha_1}$. The plot shows how the parameter value changes the spacing and shape of the streamlines compared to the case $\lambda = 0$.

Figure 9 demonstrates distorted streamlines, revealing the destabilizing influence of the second-grade fluid parameter on flow structure.

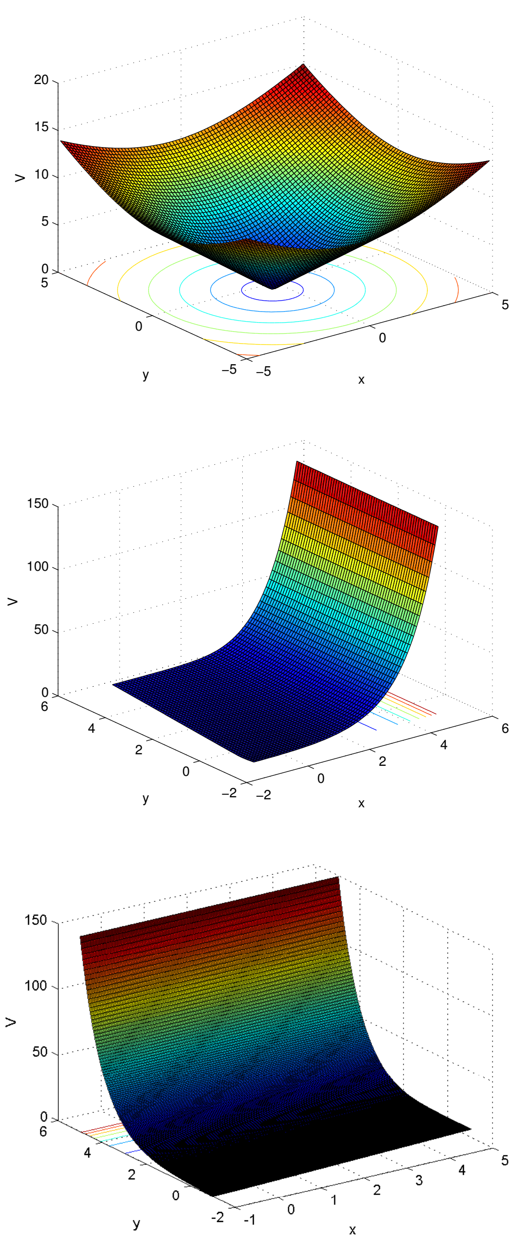

Figure 10: Velocity profiles for $\psi(x, y) = g(x) + h(y)$ in case 6.4 with $\lambda = 0$. The plot shows how the flow velocity changes across the domain when λ is zero.

Figure 10 indicates smooth and bounded velocity profiles, suggesting that the absence of λ stabilizes the flow under rotational effects.

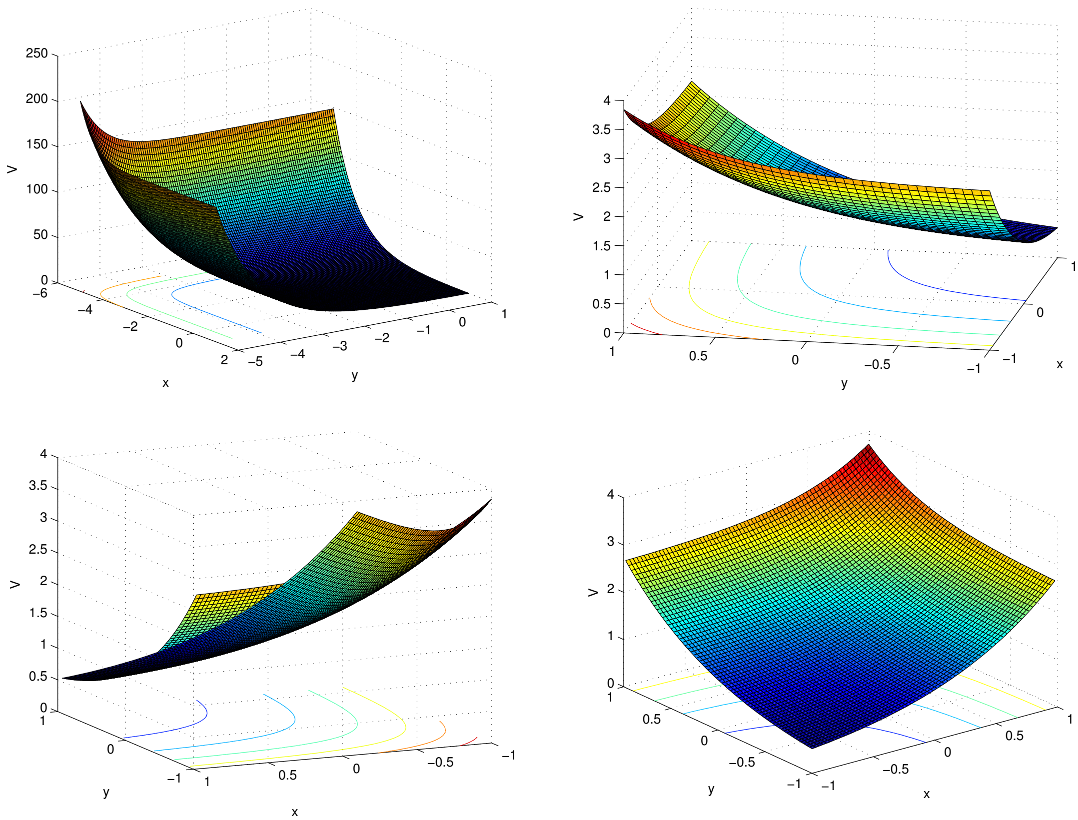

Figure 11: Velocity profiles for $\psi(x, y) = g(x) + h(y)$ in case 6.4 with $\lambda = \frac{(\rho - \mu f^2)^2}{4\alpha_1}$. The plot shows how this parameter changes the velocity pattern compared to the case $\lambda = 0$.

Figure 11 shows enhanced velocity gradients, signifying the strong coupling between viscoelasticity and magnetic forces.

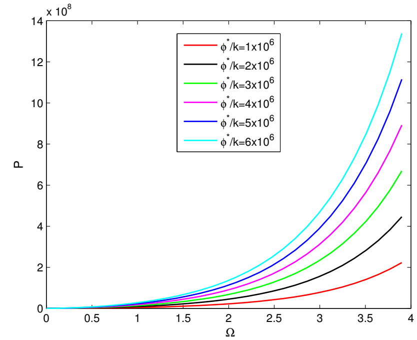

Figure 12: Variation of fluid pressure with angular velocity for different porosity values ($\frac{\phi^*}{k}$), higher porosity produces a sharper nonlinear rise in pressure as angular velocity increases.

Figure 12 highlights that pressure rises rapidly with angular velocity as porosity resistance increases, confirming the damping role of porous media.

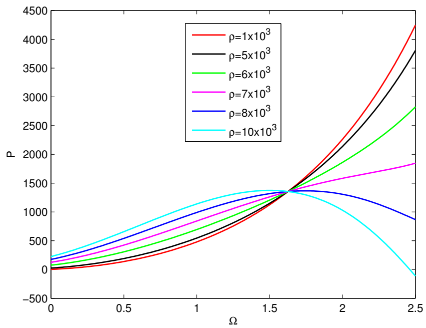

Figure 13: Change in pressure versus angular velocity for fluids of different density ρ for constant porosity $\frac{\phi^*}{k}$, showing pressure converging at $\Omega \approx 1.6$, indicating a critical rotational speed.

Figure 13 reveals that pressure initially increases and then decreases with angular velocity for higher densities, indicating competing rotational and inertial effects.

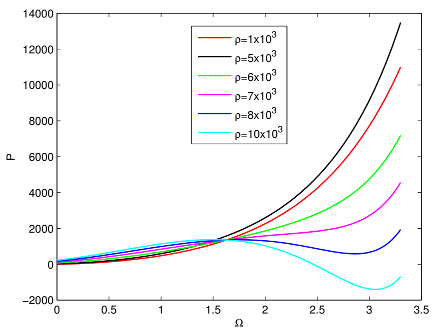

Figure 14: Change in pressure versus angular velocity for fluids of different density ρ for constant porosity $\frac{\phi^*}{k}$, showing pressure converging at $\Omega \approx 1.6$, indicating a critical rotational speed and also a rise in pressure after $\Omega \approx 3$,

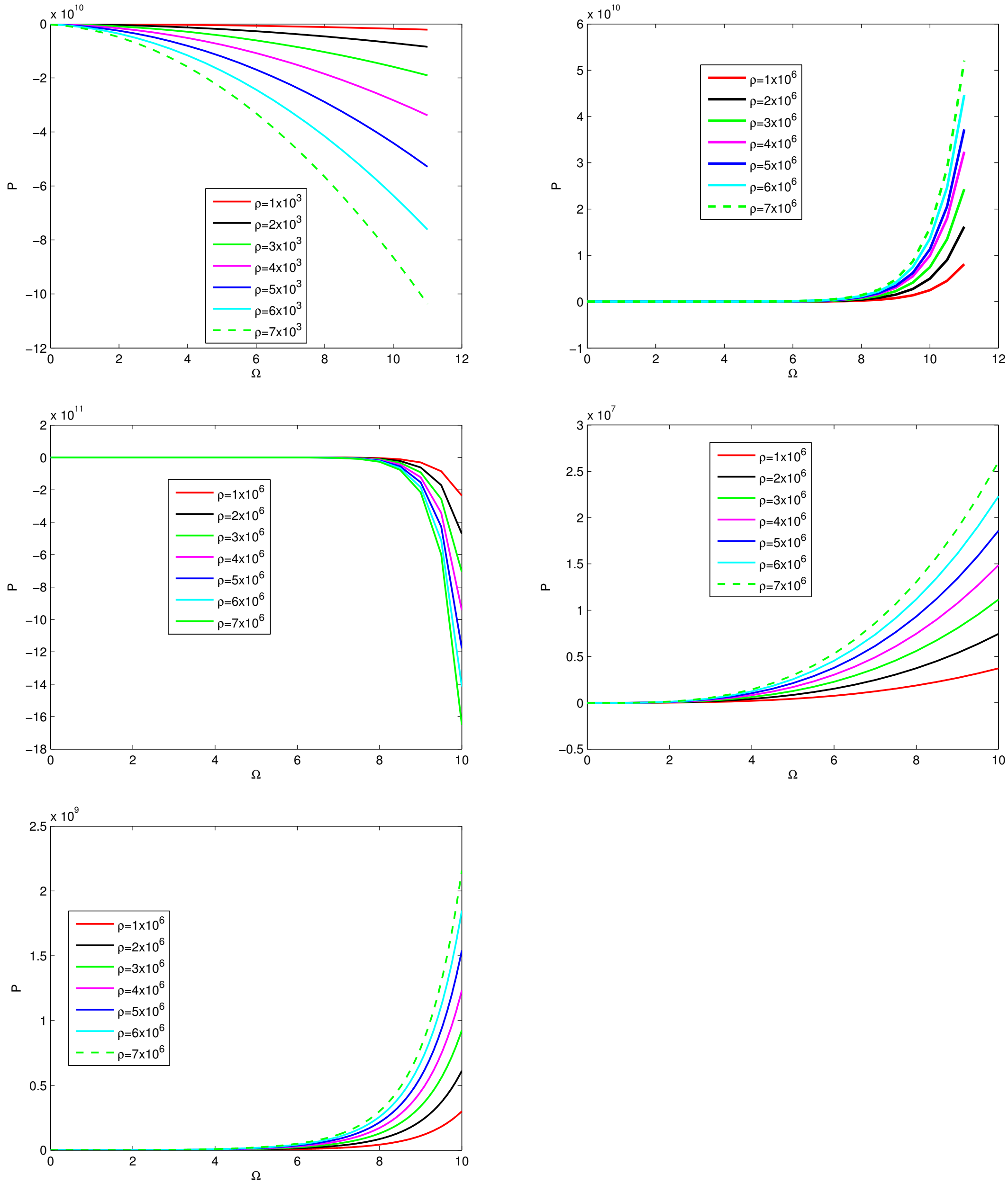

Figure 15: Pressure variation for $\psi(x, y) = g(x) + h(y)$ for case 6.4 of different density for $\lambda = 0$ depicting that in most cases, pressure increases with Ω, showing rotational dominance.

Figure 14 shows convergence of pressure curves at higher angular velocities, suggesting a saturation of rotational influence at large λ.

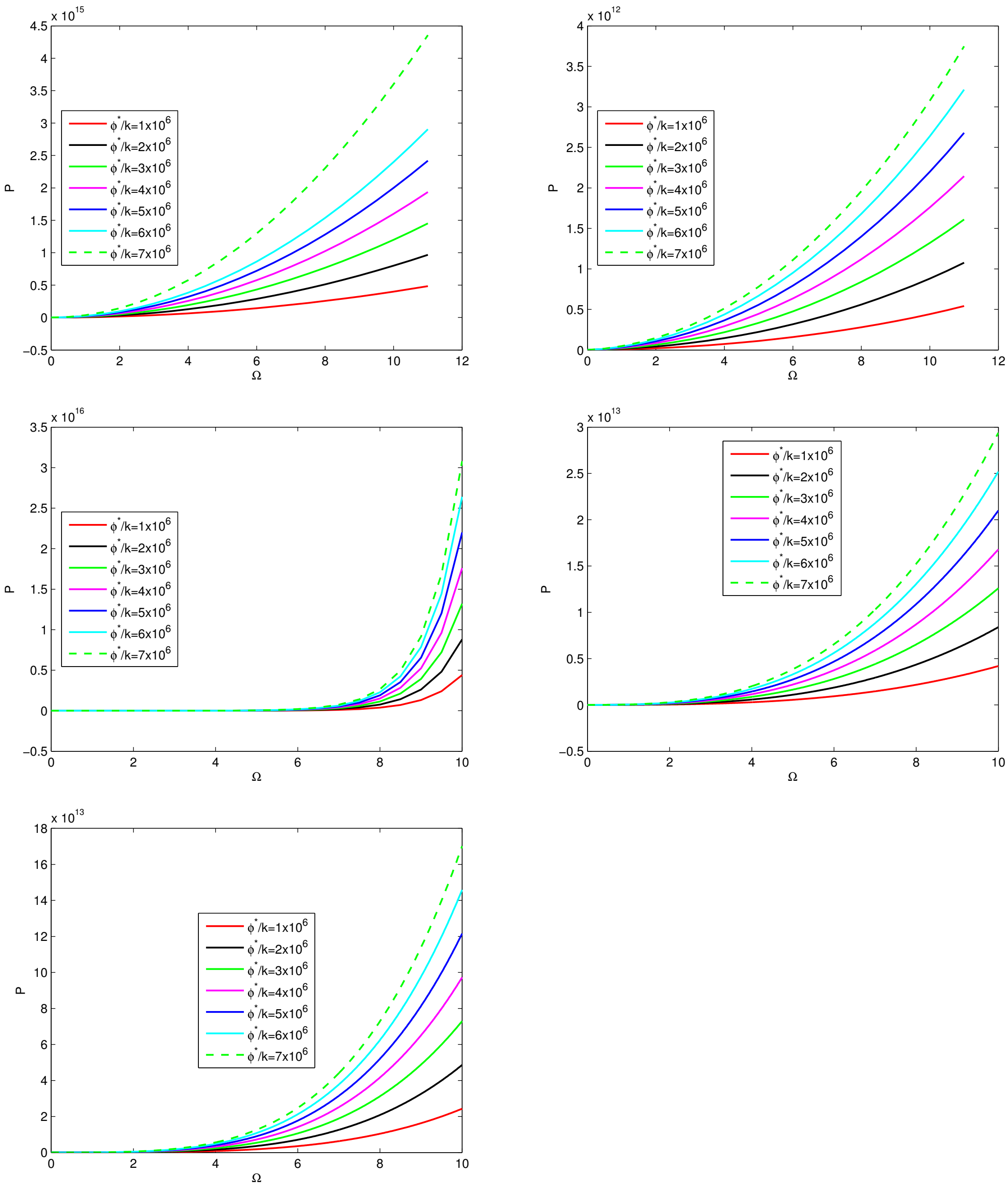

Figure 16: Pressure variation $\psi(x, y) = g(x)+h(y)$ for case 6.4 of varying porosity for $\lambda = 0$, showing pressure increases nonlinearly with angular velocity Ω, highlighting the retarding influence of the porous medium.

The subcases correspond to different vorticity–stream function couplings. In most cases, pressure increases with angular velocity λ, indicating rotational dominance, while in a few cases it decreases due to stronger viscous or elastic effects. For varying porosity parameter $\frac{\phi^*}{k}$, pressure consistently increases with λ, confirming the retarding influence of the porous medium

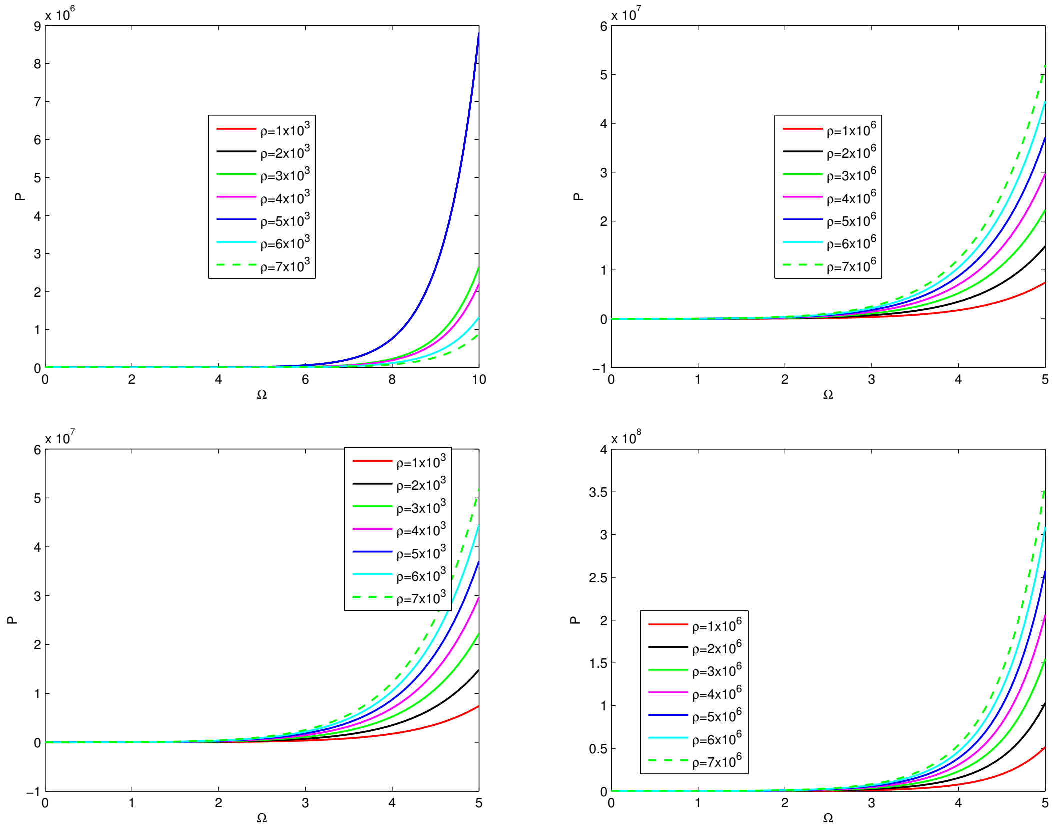

Figure 17: Pressure variation $\psi(x, y) = g(x)+h(y)$ for case 6.4 of different density for $\lambda = \frac{(\rho-\mu^* f^2)^2}{4\alpha_1}$, showing that higher density intensifies the nonlinear pressure rise with angular velocity Ω

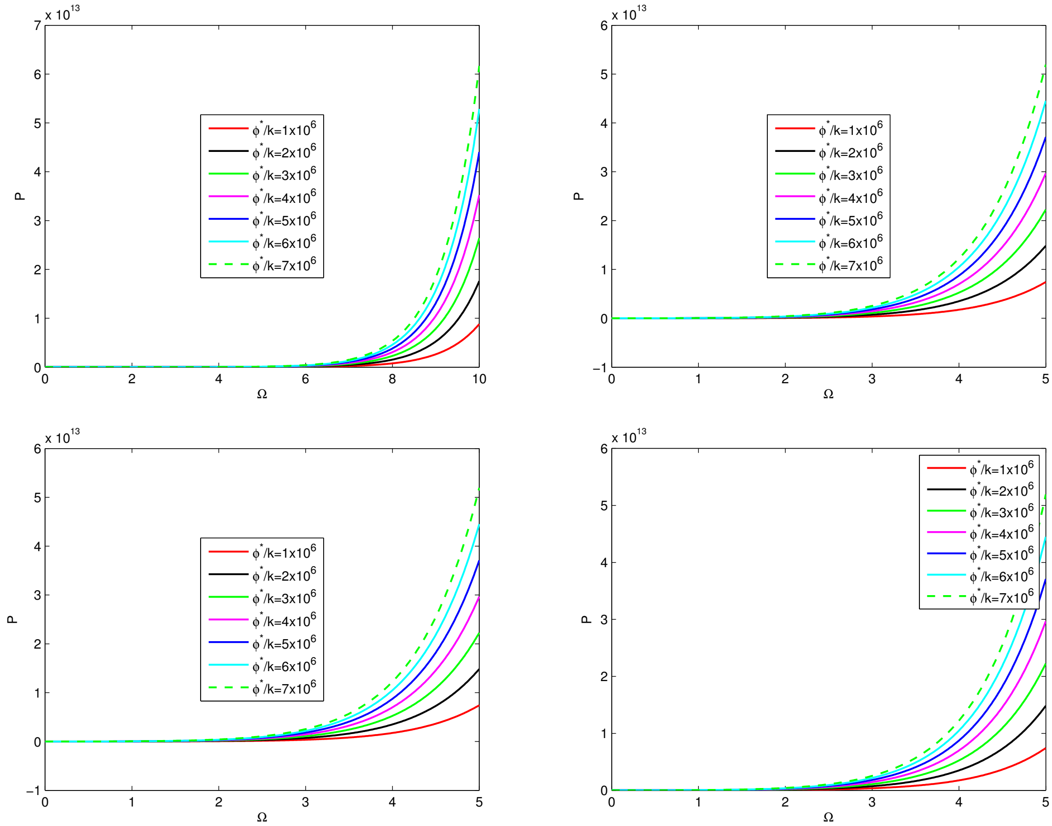

Figure 18: Pressure variation $\psi(x, y) = g(x)+h(y)$ for case 6.4 of varying porosity for $\lambda = \frac{(\rho-\mu^* f^2)^2}{4\alpha_1}$, showing porous resistance increase pressure with angular velocity Ω.

Figures in 17 and 18 shows when λ depends on fluid properties, second-grade elasticity enhances pressure growth. Increasing fluid density and porous resistance further amplify pressure with angular velocity Ω, demonstrating that non-Newtonian effects strengthen rotational stabilization.

7. Conclusions

In the current study, the inverse method has been employed to determine exact solutions for the unsteady plane, second-grade, aligned electrically conducting MHD rotating fluid flow through porous media under the influence of a magnetic field. These exact solutions are derived by assuming specific forms of the vorticity function *a priori* and the stream function a *priori*. Expressions for the velocity components, magnetic field components, stream function, vorticity functions, and pressure are obtained for both steady and unsteady cases. Additionally, graphs have been plotted to illustrate the streamline patterns, velocity profiles, and variations in pressure as a function of angular velocity for different porosity levels and varying fluid densities ρ.

The key findings from this work can be summarized as follows:

- The velocity expressions do not account for the permeability of the porous medium k or the angular velocity Ω of the rotating frame.

- For $\psi(x, y) = g(x) + h(y)$ (case I), the relationship between pressure and angular velocity Ω for different values of $\frac{\phi^*}{k}$ with constant fluid density ρ indicates that pressure is directly proportional to angular velocity. The rate of increase in pressure rises with $\frac{\phi^*}{k}$.

- For $\psi(x, y) = g(x) + h(y)$ (case I) with constant $\frac{\phi^*}{k}$ and fluids of different densities ρ, the relationship between pressure and angular velocity Ω shows that pressure decreases with increasing angular velocity. The rate of decrease becomes more pronounced with higher fluid density.

- For $\psi(x, y) = g(x) + h(y)$ (case II) with fluid density ρ and a constant value of $\frac{\phi^*}{k}$ (for higher values of k), the pressure function exhibits an increase with rising angular velocity Ω.

- For $\psi(x, y) = g(x) + h(y)$ (case III) with fluids of varying densities ρ and a constant $\frac{\phi^*}{k}$, the pressure function increases and converges to a common value for all densities at an angular velocity Ω of approximately 1.6. Beyond $\Omega \approx 1.6$, the pressure initially decreases for higher densities ρ and subsequently increases. For lower densities ρ, the pressure increases very rapidly with Ω.

- For $\psi(x, y) = g(x)+h(y)$ (case IV) with varying values of ρ and a constant $\frac{\phi^*}{k}$, when $\lambda = 0$, the pressure increases with angular velocity in three subcases, as depicted in Figures 15 and decreases in two subcases. The pressure variation for different $\frac{\phi^*}{k}$ at a constant density ρ shows an increase with Ω in all subcases, as illustrated in Figure 16. For the scenario where $\lambda = \frac{(\rho-\mu^* f^2)^2}{4\alpha_1}$, the pressure increases with angular velocity for both fluids of different densities ρ at a constant $\frac{\phi^*}{k}$ and for different $\frac{\phi^*}{k}$ at a constant density ρ can be shown in the figure 17 and 18.

References

[1] Aich, W., Abbas, A., Obalalu, A. M. et al., Double diffusive MHD stagnation point flow of second grade fluid in non-Darcy porous media under radiation effects, Sci Rep, 15 (2025), 395.

[2] Ames, W. F., Non-linear partial Differential equations in Engineering, Academic Press, New York, 1965.

[3] Asghar, S . Mohuyuddin. M. R and Siddiqui A. M., On Inverse Solution of Riabouchinsky Flows of second grade fluid, Tumsui Oxford Journal of Mathematical Sciences, 22(2) (2006), 221.

[4] Balswaroop Bhatt and Angela Shirley, Plane viscous flows in porous medium, Matematicas: Ensenanza Universitaria, 16(1) (2008), 51-62.

[5] Benharbit and Siddiqui, A. M., Certain solutions of the equations of planer motion of a second grade fluid for steady and unsteady cases, Acta Mechanicu, (1992), 85-94.

[6] Benharbit and Siddiqui, A. M., Certain solutions of the equations of planer motion of a second grade fluid for steady and unsteady cases, Mapana journal of Sciences, 2(1) (2003), 1-24.

[7] Chandna, O. P. and Oku-Ukpong, E. O., Unsteady second grade aligned MHD fluid flows, Acta Mech., 107 (1994), 77.

[8] Chandna, O. P and Oku-Ukpong, E. O., Flows for chosen vorticity function-Exact solutions of the Navier-Stokes Equations, Int. J. Math and Math. Sci., 17(1) (1994), 155.

[9] Fetecau, C., Vieru, D., On an Important Remark Concerning Some MHD Motions of Second-Grade Fluids through Porous Media and Its Applications, Symmetry, 14 (2022), 1921.

[10] Fetecau, C., Akhtar, S., Forna, N. C., Moroşanu, C., General Solutions for MHD Motions of Second-Grade Fluids Through a Circular Cylinder Filled with Porous Medium, Symmetry, 17 (2025), 319.

[11] Gupta, A. S., Ekman layer on a porous plate, The Physics of Fluids, 5 (1972), 930-931.

[12] Hui, W .H., Exact solutions of the unsteady two dimensional Navier-Stokes equations, ZAMP, 38 (1987), G89.

[13] Hussan Z., Kamal S., Manar Alqudah, Thabet Abdeljawad, Variable thermal conductivity effects on MHD flow of non-Newtonian ternary hybrid nanofluid between rotating disks, A Cattaneo–Christov heat transfer analysis, Case Studies in Thermal Engineering, 71 (2025), 106119.

[14] Imran, M. and Fetecau, C., MHD oscillating flows of a rotating second grade fluid in porous medium, Communication in Nonlinear Science and Numerical Simulation, (2014), 1-12.

[15] Jeffery, G. B., On the two dimensional steady motion of a viscous fluid, Phil. Mag., 29 (1915), 455.

[16] Kamal, M., Ali, F., Khan, N. et al., Second law analysis of two phase Maxwell mixed convective nanofluid using Marangoni flow and gyrotactic microorganism framed by rotating disk, J. Therm Anal Calorim, 150 (2025), 1947–1966.

[17] Kovasznay, L. I. G., Laminar flow behind a two dimensional grid, Proc. Cambridge Phil. Soc., 44 (1948), 58.

[18] Kumar, M. Sil, S. and Sharma R., Solutions of unsteady second grade aligned MHD fluid flow having prescribed vorticity distribution function, Bul. Cal. Math. Soc., 105(6) (2013), 445.

[19] Kumar, M. Sil, S. and Thakur, C., Some exact solutions for the flow of a second grade MHD fluid via prescribed vorticity, Acta Ciencia Indica, 45(1) (2014), 123.

[20] Labropulu, F., Exact solutions of a non-Newtonian fluid flows with prescribed Vorticity, Acta Mechanica, 141 (2000a), 110.

[21] Labropulu, F., A few more exact solutions of a second grade fluid via inverse method, Mechanics Research Communication, 27(6) (2000), 713.

[22] Labropulu. F., Generalized Beltrami flows and other closed form solutions of an Unsteady Viscoelastic Fluid, JMMS, 30(5) (2002), 271.

[23] Labropulu, F., A few more exact solutions of a second grade fluid via inverse method, Mechanics Research Communication, 27(6) (2000), 713.

[24] Mishra R B, Mishra P, Srivastava A. K and Thakur C., Some exact solutions of second grade aligned magnetohydrodynamic flow in porous media, IJMA, 2(4) (2011), 589.

[25] Naeem, R. K., Exact solutions of second-grade fluid via inverse method, Journal of Basic and Applied Sciences, 7(1) (2011), 27.

[26] Naeem, R. K., Younus, S., and Dania, Inverse solutions for unsteady incompressible couple stress fluid flows, Int. J. of Math and Mech., 6(5) (2010), 1.

[27] Rajagopal, K. R. and Gupta, S., On class of exact solutions to the equations of motion of a second grade fluid, Int. J. Eng. Sci., 19 (1981), 1009.

[28] Ram, G. and Mishra, R. S., Unsteady MHD flow of fluid through porous medium in a circular pipe, Indian Journal Pure and Applied Mathematics, 8(6) (1977), 637-647.

[29] Rashid, A. M., Effects of radiation and variable viscosity on unsteady MHD flow of a rotating fluid from stretching surface in porous media, Journal of Egyptian Mathematical Society, 2(1) (2014), 134-142.

[30] Ridha, S., and Abdulhadi, A., Unsteady heat transfer analysis on the MHD flow of a second grade fluid in a channel with porous medium, Iraqi Journal of Science, 54(1) (2023), 174-181.

[31] Rivlin, R. S. and Ericksen J. L., On Inverse Solution of Riabouchinsky Flows of second grade fluid, Stress deformation relations for isotropic materials, 4 (1955), 323.

[32] Siddiqui, A. M. and Kaloni, P. N., Certain inverse solutions of non-Newtonian fluid, Int. J. Nonlinear Mech, 21 (1986), 439.

[33] Singh, S., Singh, H. and Babu, R., Hodograph transformations in steady plane rotating hydromagnetic flow, Astrophysics and Space Science, 106 (1984), 231-243.

[34] Singh, K. K., and Singh, D. P., Steady plane MHD flows through porous media with constant speed along each stream line, Bulletin of Calcutta Mathematical Society, 85(3) (1993), 255-262.

[35] Singh B. and Thakur C., An exact solution of plane unsteady MHD non-Newtonian fluid flows, Indian. J. Pure. Appl. Math., 33(7) (2002), 993.

[36] Sil, S. and Kumar, M., A lass of solution of orthogonal plane MHD flow through porous media in a rotating frame, Global Journal of Science Frontier Research: A Physics and Space Science, 14(7) (2014), 17-26.

[37] Sil, S. and Kumar, M., Exact solution of second grade fluid in a rotating frame through porous Media using Hodograph transformation method, Journal of Applied Mathematics and Physics, 3(11) (2015), 1443.

[38] Sil, S., Kumar, M. and Thakur, C., Solutions of non-Newtonian MHD transverse fluid flows through porous media, Proceedings of 57th Congress of ISTAM, An International Meet. Defence Institute of Advanced Technology, Pune, India, (2012), 17-20.

[39] Soundalgekar, V. M. and Por. I., On hydromagnetic flow in a rotating fluid past an infinite porous wall, Zeitschrift Angewandte Mathematik und Mechanik, 53 (1973), 718-719.

[40] Taylor, G. I., On decay of vorticities in a viscous fluid, Phil. Mag., 46(6) (1923), 671.

[41] Thakur, C. and Mishra, R. B., On steady Plane Rotating Hydromagnetic flows, Astrophysics and Space science, 146(1) (1988), 89-97.

[42] Thakur, C. and Singh, B., Study of variably inclined MHD flows through porous media in magnetograph plane. Bulletin of Calcutta Mathematical Society, 92 (2000), 39-50.

[43] Thakur, C., Kumar, M., and Mahan, M., Exact solution of steady MHD orthogonal plane fluid flows through porous media, Bulletin of Calcutta Mathematical Society, 98 (2006), 583-596.

[44] Tobak. M. and Lin, S. R., On Inverse Solution of Riabouchinsky Flows of second grade fluid, AlAAJ, 24 (1986), 334.

[45] Wang. C. Y., On a class of exact solutions of the Navier-Stokes equations, J. of Appl. Mech., 33 (1966), 696.

[46] Wang, C .Y., Exact solutions of the steady-state Navier-Stokes equations, Anrau. Rev. Fluid. Mech., 23 (1991), 159.

[47] Zeb, S., et al., Melting heat transfer and thermal radiation effects on MHD tangent hyperbolic nanofluid flow with chemical reaction and activation energy. THERMAL SCIENCE: Year, Vol. 27, Special Issue 1 (2023), S253-S261.